Regulation of the Human Prostacyclin Receptor Gene by the Cholesterol-responsive Sterol Response Element Binding Protein (SREBP) 1.

Elizebeth C. Turner and B. Therese Kinsella*

UCD School of Biomolecular and Biomedical Sciences, UCD Conway Institute of Biomolecular and Biomedical Research, University College Dublin, Belfield, Dublin 4, Ireland.

*Corresponding author: Tel: 353-1-7166727; Fax 353-1-7166456
Email: Therese.Kinsella@ucd.ie

Running Title: Prostacyclin Receptor Gene Regulation by SREBP1

Acknowledgements: This work was supported by the Programme for Research in Third Level Institutions (PRTLI) 5 and Science Foundation Ireland.

Conflict of Interest: none declared

Abstract.
Prostacyclin and its prostacyclin receptor, the IP, play essential roles in regulating haemostasis and vascular tone and have also been implicated in a range cardio-protective effects, but through largely unknown mechanisms. In this study, the influence of cholesterol on human (h)IP gene expression was investigated in cultured vascular endothelial and platelet-progenitor megakaryocytic cells. Cholesterol-depletion increased hIP mRNA, hIP promoter-directed reporter gene expression and hIP-induced cAMP generation in all cell types. Furthermore, the constitutively active SREBP1a, but not SREBP2, increased hIP mRNA and promoter-directed gene expression while deletional and mutational analysis uncovered an evolutionary conserved sterol-response element (SRE), adjacent to a known functional Sp1 element, within the core hIP promoter. Moreover, chromatin immunoprecipitation assays confirmed direct cholesterol-regulated binding of SREBP1a to this hIP promoter region *in vivo,* while immunofluorescence microscopy corroborated that cholesterol-depletion significantly increases hIP expression levels. In conclusion, the hIP gene is directly regulated by cholesterol-depletion that occurs through binding of SREBP1a to a functional SRE within its core promoter. Mechanistically, these data establish that cholesterol can regulate hIP expression which may, at least in part, account for the combined cardio-protective actions of low serum cholesterol through its regulation of prostacyclin receptor (IP) expression within the human vasculature.

Key Words: Prostacyclin Receptor, gene expression, transcription, Sterol-response element (SRE), promoter, sterol-response element binding protein (SREBP).

Abbreviations: bHLH-LZ, basic helix-loop-helix -leucine zipper; ChIP, chromatin immunoprecipitation; COX: cyclooxygenase; CVD, cardiovascular disease; DMSO, dimethyl sulfoxide; ERE, estrogen response element; FBS, fetal bovine serum; HEL, human erythroleukemia; hIP, human prostacyclin receptor; IgG, immunoglobulin G; IP, prostacyclin receptor; RLU, relative luciferase unit; SEM, standard error of the mean; SRE, sterol-response element; SREBP, sterol-response element binding protein; TI, transcription initiation; SDM, site-directed mutagenesis; URR, upstream repressor region.

Introduction

The prostanoid prostacyclin, or prostaglandin (PG) I_2, plays an essential role in haemostasis and in the regulation of vascular tone, acting as a potent *anti*-thrombotic and vasodilatory agent (1-3). The actions of prostacyclin are primarily mediated through the I Prostanoid receptor or, in short, the IP, a G protein-coupled receptor (GPCR) predominantly coupled to Gs-mediated activation of adenylyl cyclase (1-3). The human (h) IP is subject to complex post-translational lipid modifications (4,5) and to regulation by a range of interacting proteins (6-10). For example, it undergoes agonist-induced internalization through a Rab5a-dependent mechanism, with subsequent recycling to the plasma membrane involving a direct interaction between the hIP and Rab11a to dynamically regulate the cellular responses to prostacyclin *in vivo* (6,7,9). The hIP also directly interacts with the HDL receptor/scavenger receptor class B type 1 (SR-B1) adaptor protein 'PDZ domain-containing protein 1 (PDZK1)' and this interaction is essential for prostacyclin-induced endothelial cell migration and *in vitro* angiogenesis (8).

Consistent with this and with its actions within the vasculature, imbalances in the levels of prostacyclin or of prostacyclin synthase or the IP have been implicated in a range of cardiovascular disorders (11-13) and, clinically, prostacyclin analogues are used in the treatment of pulmonary arterial hypertension (14). Prostacyclin also acts as a critical cardio/cytoprotective agent during acute myocardial ischemia (15-17) and enhances endothelial cell (EC) survival supporting neovascularization (18). Several single nucleotide polymorphisms occur in the hIP gene that correlate with receptor dysfunction including enhanced platelet activation in deep vein thrombosis and increased intimal hyperplasia (19-21) and, more recently, with increased occurrence of major obstruction in patients with coronary artery disease (19,22,23). In keeping with this, $IP^{-/-}$ null mice display increased tendency towards thrombosis, intima hyperplasia, atherosclerosis and restenosis (24-28), while endothelial progenitor cells (EPCs) from $IP^{-/-}$ fail to undergo re-endothelialization in response to vascular injury, highlighting the central role of the IP in limiting neointima hyperplasia/restenosis (29). Interestingly, the female hormone estrogen enhances the expression of cyclooxygenase (COX) 1, COX2 and prostacyclin synthase, resulting in a six-fold increase in systemic prostacyclin levels (30,31). Furthermore, the atheroprotective effects of estrogen seen in female low-density lipoprotein receptor null mice ($LDLR^{-/-}$) are abrogated in double $LDLR^{-/-}/IP^{-/-}$ knockout mice (30). Collectively, these latter findings strongly suggested that some of the cardioprotective effects of estrogen are mediated through the IP (30,31). Consistent with this, we recently discovered that expression of the hIP gene is up-regulated by estrogen, that occurs through a transcriptional mechanism involving binding of the estrogen receptor (ER)α, but not ERβ, to a highly conserved estrogen response element (ERE) identified within the hIP promoter (32).

The clinical benefits of low plasma LDL-cholesterol in the prevention of coronary artery disease are also widely recognized and can, in part, be accounted for by improvements in endothelial-dependent vasodilation by prostacyclin and nitric oxide (33). For example, Statins yield pleiotropic beneficial effects not associated with their cholesterol lowering properties (34,35), most notably improved cerebral blood flow associated with enhanced nitric oxide generation (36,37). In terms of prostacyclin, reductions in LDL-cholesterol increase prostacyclin generation in ECs by transcriptional upregulation of COX2, but not COX1 or prostacyclin synthase, and occurs through binding of the cholesterol-responsive transcription factor 'sterol response element binding protein (SREBP)' to a sterol response element (SRE) within the COX2 promoter (38,39). The finding that reduced LDL-cholesterol selectively modulates COX2 expression, without corresponding changes in COX1 or prostacylin synthase levels, led us to hypothesize that the increased COX2-derived generation of prostacyclin may be accommodated by and/or, in theory, may be further benefited if there were a corresponding upregulation of IP expression levels.

Hence, the overall aim of this study was to establish whether alterations in cholesterol levels actually regulate expression of the hIP. Herein, it was established that depletion of cholesterol led to significant increases in IP gene expression in cultured vascular ECs and in platelet-progenitor human erythroleukemic (HEL) cells and that this occurred through binding of SREBP1a, but not SREBP2, to a highly conserved SRE *cis*-acting element discovered within the 'core hIP promoter'. Collectively, the data provides compelling evidence that the hIP gene is a *bone fide* target for regulation by the cholesterol-responsive transcription factor SREBP1a within the vasculature and, thereby, presents additional mechanistic insights into the potential cardio-protective actions of reduced serum cholesterol through its ability to regulate the synthesis and actions of prostacyclin, through its transcriptional regulation of COX2 (39) and of the IP, respectively.

Results

Cholesterol regulation of human IP expression in EA.hy926 and HEL cells

Some of the clinical benefits of low LDL-cholesterol within the CV system have been linked with improvements in endothelium-dependent effects of both prostacyclin and nitric oxide (3,33). Moreover, reductions in LDL-cholesterol leads to dose-dependent increases in prostacyclin generation through its transcriptional up-regulation of COX2, involving binding of the cholesterol-responsive SREBP1a to a sterol response element (SRE) within the COX2 promoter (39). Hence, the rationale for this study was to investigate whether cholesterol may regulate human (h) IP expression, obtaining additional mechanistic insights into some of the cardio-protective effects of reduced LDL-cholesterol through its regulation of prostacyclin synthesis and function.

Initially, RT-PCR analysis was used to examine possible regulation of hIP mRNA expression by cholesterol in the human endothelial EA.hy926 (**Figure 1A)** and megakaryocytic HEL 92.1.7 (**Supplemental Figure 1A**) cell lines, where the non-responsive GA3'PDH transcript served as controls. More specifically, to monitor responsiveness to cholesterol, cells were cultured in media containing normal serum (NS; 10% FBS); low cholesterol serum (LCS; 10% delipidated FBS) or high cholesterol serum (HCS; 10% FBS supplemented with 10 µg/ml cholesterol and 1 µg/ml 25-hydroxycholesterol), essentially as previously described (39). Quantitative real-time RT-PCR analysis established that LCS increased hIP mRNA expression in EA.hy926 (2-fold, $P = 0.0003$; **Figure 1B**) and HEL (1.3-fold, $P = 0.008$; **Supplemental Figure 1B**) cells, while pre-incubation with the transcriptional inhibitor actinomycin D (ActD), but not with the translational inhibitor cycloheximide (CHX), completely abrogated the LCS-induction of hIP mRNA expression in both cell lines (**Figure 1B & Supplemental Figure 1B**, respectively). Culturing cells in HCS did not significantly affect hIP mRNA expression in either cell type while neither HCS nor LCS affected GA3'PDH mRNA expression (**Figure 1A & 1B** and **Supplemental Figure 1A & 1B**).

Previous studies have defined the human IP promoter, hereinafter denoted PrmIP, as nucleotides -2449 to -772 relative to the translational start codon (+1) within the hIP gene (40). Herein, genetic reporter assays were used to examine PrmIP-directed luciferase gene expression as a function of serum cholesterol levels (NS, LCS or HCS). Culturing of EA.hy926 and HEL cells in LCS led to 3-fold ($P < 0.0001$) and 1.4-fold ($P = 0.006$) inductions in PrmIP-directed luciferase gene expression, respectively, relative to those levels in NS (**Figure 1C & Supplemental Figure 1C**, respectively). Conversely, in HCS, there was modest, but significant, decreases in PrmIP-directed luciferase expression in EA.hy926 (1.2-fold, $P = 0.024$; **Figure 1C)** and HEL (1.2-fold, $P = 0.036$; **Supplemental Figure 1C**) cells.

As stated, the hIP is primarily coupled to Gs-mediated adenylyl cyclase activation leading to agonist-dependent increases in cAMP generation (2). Hence, the effect of culturing EA.hy926 and HEL cells in NS, LCS or HCS on agonist-induced cAMP generation following stimulation of cells with the selective IP agonist cicaprost was also examined. Culturing EA.hy926 (**Figure 1D & 1E;** $P = 0.0021$, ANOVA**)** and HEL (**Supplemental Figure 1D & 1E;** $P = 0.003$, ANOVA) cells in LCS also resulted in approximately 3-fold increases in agonist (cicaprost)-induced cAMP generation relative to that in NS or HCS, confirming functional increases in hIP expression in response to reduced serum cholesterol in both cell types.

Taken together these data establish that depletion of serum cholesterol influences hIP gene expression through up-regulation of hIP mRNA, PrmIP-directed gene expression in addition to enhancing functional expression of the hIP, promoting agonist-induced cAMP generation, in both cultured vascular ECs and in megakaryocytic HEL cells and that this occurs at the transcriptional level in both cell types.

Identification of a functional SRE within the PrmIP

Thereafter, 5' deletional analysis of PrmIP in combination with genetic reporter-analyses was used to localize the cholesterol-responsive region(s) within PrmIP in both EA.hy926 and HEL cells. Initially, consistent with previously reported data (32,40), progressive 5' deletion of PrmIP identified the 'core promoter", defined as the minimal promoter unit required for basal transcriptional activity, at -1042 to -917 and an upstream repressor region (URR) at -1783 to -1704 in EA.hy926 cells cultured under basal conditions in NS (**Figure 2A**). In cells cultured in LCS, cholesterol depletion

resulted in ~ 3-fold inductions in luciferase expression directed by the PrmIP-, PrmIP1-, PrmIP2-, PrmIP3-, PrmIP4-, PrmIP5- and PrmIP6- subfragments ($P < 0.0001$ in all cases; **Figure 2A**) but did not affect luciferase expression directed by the smallest PrmIP7-subfragment devoid of the core promoter region. More specifically, deletion of nucleotides -1042 to -917 completely abrogated the increased PrmIP-directed luciferase gene expression observed on culturing EA.hy926 cells in LCS and, thereby, localized the cholesterol-responsive region to the proximal 'core promoter' region of PrmIP (**Figure 2A**). Similarly, and consistent with previous reports (32,40,41), culturing HEL cells under basal conditions in NS confirmed that the 'core promoter' was localized to -1042 to -917 but that an URR in this cell type was identified between -1524 to -1293, as opposed to the functional URR identified in EA.hy926 cells between -1783 to -1704 (Compare NS data in **Supplemental Figure 2A to Figure 2A**). However, it was found that culturing of HEL cells in LCS led to 1.4-fold inductions in luciferase expression by PrmIP and by each of its subfragments PrmIP1-PrmIP6, but not by the smallest subfragment PrmIP7 (**Supplemental Figure 2A**).

It has been previously established that hIP gene expression is transcriptionally regulated by the co-ordinate binding of Sp1, PU.1 and Oct-1 to their *cis*-acting elements within the 'core promoter' region of PrmIP (40). Herein, bioinformatic analyses (42) also revealed a putative sterol response element (SRE) within the 'core promoter', where the 5' nucleotide of the SRE is at -937 (**Figure 2B**). Moreover, the SRE element is evolutionary conserved (**Figure 2B**) and, by way of example, 9/10 residues of the SRE in the hIP gene are identical to those of the consensus SRE of the HMG CoA synthase gene (**Figure 2C**). Hence, luciferase expression-directed by PrmIP and by PrmIP6, the smallest subfragment containing the cholesterol-responsive core promoter, or -directed by PrmIP6 derivatives carrying mutated SP1*, PU.1*, Oct-1* and SRE* *cis*-acting elements was examined following culturing EA.hy926 cells in NS and LCS. In LCS, there were 3-fold inductions in luciferase expression directed by PrmIP and PrmIP6 ($P < 0.0001$ in each case; **Figure 2D & 2E**). Consistent with previous reports (40), mutation of the individual PU.1*, Oct-1* and Sp1* elements in PrmIP6 each led to significant reductions in luciferase expression in EA.hy926 cells cultured in NS (**Figure 2D**). However, the PU.1* and Oct-1* mutations did not affect the LCS- induction of PrmIP6-mediated luciferase expression in EA.hy926 cells cultured in LCS (3-fold increases; $P < 0.0001$ in each case; **Figure 2D & 2E**). In contrast to this, mutational disruption of the Sp1* element in PrmIP6 led to a modest, but significant, effect reducing the induction in luciferase gene expression observed in LCS from 3-fold by PrmIP6 to 2.7-fold by the equivalent PrmIP6 subfragment containing the mutated Sp1* ($P < 0.002$; **2D & 2E**). While mutation of the SRE* element within PrmIP6 did not affect luciferase gene expression in EA.hy926 cells cultured in NS (basal data), it reduced the enhanced expression/induction in LCS from 3-fold by PrmIP6 to only 1.3-fold by the equivalent PrmIP6 subfragment carrying the mutated SRE* element ($P < 0.047$; **Figure 2D & 2E**). Furthermore, combined mutation of the SRE* and Sp1* elements in PrmIP6 completely abolished the induction in luciferase expression in LCS ($P < 0.827$; **Figure 2D & 2E**).

Similarly, these data in EA.hy926 cells were fully corroborated by studies in HEL cells, whereby it was established that disruption of the SRE, and to a lesser extent, the Sp1 elements impaired the LCS-mediated induction of PrmIP6-directed reporter gene expression, while mutation of neither the PU.1 nor the Oct1 elements had any significant affect (**Supplemental Figure 2B & 2C**). Taken together, these data have identified a consensus SRE, located at -937 within the 'core promoter', that is critical for increased PrmIP-directed gene expression that occurs following culturing of EA.hy926 or HEL cells in LCS-containing media. Furthermore, it has also identified a minor role for Sp1 in this regulation in both cell types.

Determination of SREBP Specificity

In general, the lipid-responsive SREBP-1 and -2 act as master regulators of a host of hepatic and extra-hepatic genes associated with lipid metabolism, including uptake and/or *de novo* synthesis of cholesterol (43,44). SREBP-1a is a strong transcriptional activator of many cholesterol-responsive genes whereas its splice variant SREBP1c has a shorter transactivation domain and, therefore, is less transcriptionally active (45). SREBP2 is encoded by a distinct gene and preferentially regulates expression of genes involved in cholesterol homeostasis (46). In general, as depicted in the model in **Figure 6A**, SREBPs remain sequestered in the endoplasmic reticulum (ER) where they exist as transcriptionally inactive precursors complexed with SREBP cleavage-activating protein (SCAP).

Under low cholesterol conditions, SCAP escorts the SREBP to the Golgi apparatus where it is cleaved by two specific proteases, namely by site 1 protease (S1P) and S2P, releasing the cleaved N-terminal 'bHLH-LZ domains' of the given SREBP. The transcriptionally active 'bHLH-LZ domains', in turn, translocate to the nucleus where they transactivate gene expression by binding to SREs within target promoters (45,47,48).

Hence, herein, the specificity of SREBP1a or SREBP2 to regulate PrmIP-directed gene expression was investigated by ectopic expression of the constitutively active SREBP1a^{-460} and SREBP2^{-468}, corresponding to their aforementioned bHLH-LZ domains, respectively (49). Over-expression of constitutively active SREBP1a^{-460}, but not SREBP2^{-468}, substantially increased hIP mRNA expression in both EA.hy926 ($P < 0.0001$; **Figure 3A & Supplemental Figure 3A**) and HEL cells (**Supplemental Figure 3B & 3C**) when cultured in NS. Consistent with these findings, over-expression of SREBP1a^{-460}, but not SREBP2^{-468}, also resulted in 3.5-fold and 3-fold inductions in both PrmIP- and PrmIP^{Sp1*}-directed luciferase expression in EA.hy926 cells ($P < 0.0001$; **Figure 3C**) and in HEL cells ($P < 0.0001$; **Supplemental Figure 3D**), respectively. Furthermore, neither the constitutively active SREBP1a^{-460} nor SREBP2^{-468} had any effect on reporter gene expression directed by PrmIP6 subfragments containing the mutated SRE* or PrmIP7 in EA.hy 296 cells (**Figure 3C)** or in HEL cells (**Supplemental Figure 3D**). In all cases, western blot analysis confirmed that both SREBP1a^{-460} and SREBP2^{-468} were over-expressed, and to equivalent levels, in EA.hy926 and HEL cells, where back blotting for the ubiquitously expressed HDJ-2 chaperone protein confirmed uniform protein loading in both cell types (**Figure 3B** & data not shown, respectively).

To investigate whether endogenous SREBP1 can actually bind *in vivo* to the SRE within the 'core promoter' region, chromatin immunoprecipitation (ChIP) assays were carried out on chromatin extracted from EA.hy926 cells cultured in either NS, LCS or HCS media using *anti*-SREBP1 antibodies and PCR primers to amplify the region surrounding the SRE and Sp1 *cis*-elements within PrmIP or, as controls, to amplify a genomic region located some ~2 kB upstream of the 'core promoter' (**Figure 4A, schematic**). In parallel, due to the role of Sp1 in both basal (40) and LCS-induced gene expression by the PrmIP (**Figure 2D & 2E**), similar ChIP assays were also carried out using an *anti*-Sp1 specific antibody. In EA.hy926 cells cultured in NS, and consistent with previously reported data (40), ChIP assays yielded specific PCR amplicons from the input chromatin and chromatin recovered from the *anti*-Sp1 immunoprecipitates but not from the control ChIPs generated using pre-immune IgG or no-antibody control precipitates (**Figure 4A**, middle panel). Similarly, this was also the case for the Sp1 ChIP assays using chromatin from EA.hy926 cells cultured in both HCS and LCS (**Figure 4A**, top and bottom panels respectively). Furthermore, real-time quantitative PCR confirmed that there was no difference in the relative abundance of the amplicons generated from the Sp1 ChIP assays using the primers surrounding the 'core promoter' region, regardless of whether the EA.hy926 cells were cultured in NS, HCS or LCS media (**Figure 4B**). In contrast, the *anti*-SREBP1 ChIP assays yielded specific amplicons from chromatin recovered from EA.hy926 cells cultured in NS and LCS, but not in HCS (**Figure 4A**), while real-time quantitative PCR confirmed that the relative abundance of amplicons generated from cells cultured in LCS was 1.5-fold greater in those cultured in NS ($P = 0.0057$; **Figure 4C**). Additionally, PCR analysis using the control primers to amplify the upstream genomic region, 5' of the 'core promoter' region, did not generate amplicons from the *anti*-Sp1 or *anti*-SREBP1 ChIP assays and irrespective of how the EA.hy926 cells were cultured, be it in NS, LCS or HCS (**Figure 4D**). Furthermore, as an additional positive control for the ChIP assays, amplicons for the cholesterol-responsive LDL receptor promoter were obtained from both the *anti*-Sp1 or *anti*-SREBP1 precipitated chromatin from EA.hy926 cells cultured in LCS (**Figure 4E**). These data are entirely consistent with the fact that both SREBP1 and Sp1 are known to play a cooperative role in regulating LDL receptor gene expression in response to cholesterol (50), similar to that discovered to occur herein for the hIP gene.

Failure to generate specific amplicons based on the core promoter region of PrmIP in the SREBP ChIP assays from cells cultured in HCS can be explained by examination of the forms of SREPB1 expressed in EA.hy926 cells cultured in HCS and LCS relative to that in NS (**Figure 4F & Supplemental Figure 4B**). More specifically, in HCS, SREBP1 is almost exclusively expressed as the transcriptionally-inactive precursor form, which cannot bind to DNA (**Figure 4F**; ~ 125 kDa), while in NS, both the precursor and proteolytically-cleaved, transcriptionally active form (~ 68 kDa) are present accounting for its ability to bind the SRE within the core PrmIP (**Figure 4F**). In contrast

to this, in LCS, SREBP1 is almost exclusively expressed as the cleaved, transcriptionally active form (**Figure 4F & Supplemental Figure 4B)**, accounting for its enhanced binding to the SRE, as identified in the SREBP1 ChIP assays (**Figure 4A & Figure 4C**). In contrast, Sp1 expression levels were unaffected, irrespective of whether cells were culture in NS, LCS or HCS media (**Figure 4A & Supplemental Figure 4A**). Furthermore, these data in EA.hy926 cells (**Figure 4**) were fully corroborated by similar findings in HEL cells (data not shown) and in 1^{o} HUVECs (see later; **Figure 5**).

While the experimental data presented thus far clearly suggest that SREBP1, but not SREBP2, plays a specific role in regulating hIP expression in both EA.hy926 and HEL cells (**Figure 3 & Supplemental Figure 3**, respectively), owing to lack of *anti*-SREBP1 antibody specificity, these data cannot actually discriminate between SREBP1a *versus* SREBP1c in mediating these effects. To address this, quantitative real-time PCR was used to determine the relative levels of SREBP1a and SREBP1c expression in both EA.hy926 and HEL cells and established that SREBP1a is the predominant SREBP1 isoform expressed, with only low levels of SREBP1c expression detected in both cell types (**Supplemental Figure 4C & 4D,** respectively).

Taken together, these data confirm that SREBP1, but not SREBP2, specifically binds to a functional SRE within the hIP promoter to mediate LCS-induction of hIP mRNA, PrmIP -expression and agonist-induced cAMP generation in both EA.hy926 and HEL cells where the more transcriptionally active SREBP1a is the predominant SREBP1 member expressed in both cell types.

Cholesterol regulation of hIP expression in 1^{o} HUVECs

Thereafter, it was sought to investigate whether the observed cholesterol-responsive, SREBP1-mediated induction of hIP mRNA and of PrmIP-directed gene expression may also occur in a more physiologically relevant model of vascular endothelial cells, namely in primary human umbilical vein endothelial cells (1^{o} HUVECs).

In brief, real-time quantitative RT-PCR confirmed up-regulation of hIP mRNA expression in 1^{o} HUVECs cultured in LCS (2.1-fold, P = 0.003; **Figure 5A**), an effect completely abrogated by pre-incubation with ActD but not CHX (**Figure 5A**). Culturing 1^{o} HUVECs in LCS also resulted in 2-3 fold increases in agonist (cicaprost)-induced cAMP generation relative to that in NS or HCS (**Figure 5B & 5C;** P = 0.0024 ANOVA), confirming functional increases in hIP expression in response to reduced serum cholesterol. Furthermore, this effect was greatly diminished in the presence of Ly294002, a phosphatidylinositol 3 kinase (PI3K) inhibitor known to inhibit SREBP activation (increased processing from the membrane bound precursor form to the mature transcription factor) in response to reduced cholesterol levels (Figure 5B & 5C; P = 0.0031) (51,52). Consistent with these findings, there was also a 2-fold induction in PrmIP-directed reporter gene expression in 1^{o} HUVECs cultured in LCS (P < 0.0001), while luciferase expression was not significantly different in HCS (P = 0.231) relative to that in NS culture media (**Figure 5D**). Consistent with data in EA.hy926 and HEL cells, mutation of the SRE* and Sp1* elements each substantially impaired the LCS-induction of luciferase expression in 1^{o} HUVECs while mutation of both *cis*-acting elements within PrmIP6 was required to completely abrogate that induction (**Figure 5D**). Furthermore, as previous, ectopic expression of constitutively active SREBP1a^{-460} led to greater than 2-fold inductions in hIP mRNA expression (P = 0.0034: **Figure 5A**) and PrmIP-directed luciferase activity (P = 0.004; **Figure 5D**) in 1^{o} HUVECs, while SREBP2^{-468} had no effect on either hIP mRNA or PrmIP-directed gene expression levels (**Figure 5A & 5D**). Immunoblot analysis confirmed that both SREBP1a^{-460} and SREBP2^{-468} were over-expressed and to equivalent levels in the 1^{o} HUVECs (**Supplemental Figure 5A)**. Moreover, ChIP analysis demonstrated that endogenous SREBP1 is capable of directly binding to the 'core promoter' region of PrmIP *in vivo* in 1^{o} HUVECs cultured in NS and LCS, but not in HCS, (**Figure 5E & 5G**) and that the enhanced binding in LCS can be explained by the increased levels of the cleaved 'transcriptionally active' form of SREBP1 available for binding (**Figure 5J and Supplemental Figure 5B**). Furthermore, ChIP analyses also confirmed binding of Sp1 and SREBP1 to the cholesterol-responsive LDL receptor promoter *in vivo* to chromatin extracted 1^{o} HUVECs cultured in LCS (**Figure 5I**), consistent with the cooperative transcriptional regulation of the LDL receptor expression by SREBP1 and Sp1 (50), while real-time quantitative RT-PCR established that SREBP1a, and not SREBP1c, is the predominant SREBP1 isoform expressed in 1^{o} HUVECs (**Supplemental Figure 5C**).

Thereinafter, indirect immunofluorescent staining with an affinity-purified *anti*-IP antisera directed to the intracellular $(IC)_2$ domain of the hIP (32) confirmed endogenous expression of the hIP, located predominantly at the plasma membrane, in 1^o HUVECs with no significant difference in the levels of expression when cells were cultured in HCS or NS (**Figure 5Ki & 5Kii and Supplemental Figure 5D**). In contrast, as indicated in **Figure 5Kii - 5Kv**, culturing the 1^o HUVECs with increasing ratios of LCS relative to decreasing NS, thereby gradually depleting cholesterol levels, resulted in dose-dependent increases in hIP expression levels (**Figure 5K & Supplemental Figure 5D**). Furthermore, consistent with previous reports (40), the antigenic IC_2 peptide completely blocked immune-detection of the hIP, thereby validating the antibody specificity (**Figure Kvi & Supplemental Figure 5D**).

Collectively, data presented herein establish that hIP expression is substantially up-regulated in response to serum cholesterol-depletion in several cell lineages derived from the human vasculature, including in model vascular endothelial and megakaryocytic lines and in 1^o HUVECs, and that this occurs through the direct binding of SREBP1a to a functional SRE element discovered within the 'core promoter' region of the hIP gene. Such up-regulation of the hIP expression by SREBP1 in situations of low cholesterol may provide, at least in part, a molecular explanation as to the role of endothelial derived factors, in this case the prostacyclin/hIP signalling paradigm, in protecting against coronary artery disease.

Discussion

Cardiovascular disease is a leading cause of morbidity and premature mortality and elevated LDL-cholesterolemia is a well recognised risk factor (53,54). Analysis of the effects of cholesterol and fatty acids on hepatic gene expression led to the discovery of a family of membrane-bound transcription factors named SREBPs and identified them as the master regulators of lipid homeostasis (48). While both SREBP1a and SREBP1c are known to activate genes involved in regulating general lipid metabolism, SREBP2 regulates expression of genes involved in cholesterol homeostasis (47,48).

Although numerous transcriptional targets of SREBPs have been identified, little is known about their effects on expression of genes in extra-hepatic tissues or genes not directly associated with lipid homeostasis. The finding that endothelial prostacyclin levels may be increased by the cholesterol-responsive SREBP1 through its transcriptional up-regulation of COX2 was the first demonstration that the SREBP-mediated pathway(s) are present in vascular tissue (38,39). However, despite the fact that cholesterol-depletion leads to SREBP-COX2-mediated increases in prostacyclin generation, to enhance endothelium-dependent vasodilator capacity but without corresponding increases in COX1 or prostacyclin synthase levels, up until this current study it was unknown whether serum cholesterol may actually influence IP expression to accommodate the increased vasodilatory responses.

Herein, culturing of cells in low serum cholesterol led to substantial up-regulation of hIP mRNA, increased PrmIP-derived gene expression and hIP-induced cAMP generation in both model vascular endothelial (EA.hy926) and megakaryocytic (HEL 92.1.7) cells and in 1^{o} HUVECs. The transcriptional inhibitor ActD, but not the translational inhibitor CHX, completely abrogated the effects of cholesterol depletion, while elevated cholesterol (HCS) did not substantially affect hIP gene expression in any of the cell types under study. Furthermore, immunofluoresence microscopy corroborated these findings and showed that, in 1^{o} HUVECs, hIP expression was increased in a dose-dependent manner in response to decreasing cholesterol conditions. Collectively, these data identify the hIP gene as a *bona fide* target for reduced cholesterol-regulation and that this regulation occurs at the transcriptional level.

SREBPs are members of the basic helix-loop-helix -leucine zipper (bHLH-LZ) class of transcription factors, and bind as dimers to a direct repeat "E-box" element referred to as a sterol response element (SRE; 5′-ATCACCCCAC-3′; **Figure 2C**; (55,56)). The first well-characterized functional SRE was that of the human LDL receptor gene promoter (57), which was then used for affinity purification and subsequent cloning of the SREBP *trans*-acting factor (58). Herein, the site of cholesterol-responsiveness was localized to -1042 to -917 within the PrmIP, and bioinformatic analysis revealed a near perfect consensus 10-bp SRE at -937 (**Figure 2B & 2C**). Genetic reporter analysis revealed that the effects of cholesterol depletion, namely increased PrmIP-directed gene expression, were significantly impaired when the SRE was mutated/disrupted. These data established that the SRE within the PrmIP is fully functional and essential for the regulation of hIP expression in response to serum cholesterol. Furthermore, the SRE was found to be highly conserved in a host of other species including in the canine, bovine and rodent IP promoters (**Figure 2B**).

Genome-wide binding profiles for SREBP1 versus SREBP2 in hepatic chromatin revealed that only 11.7 % of their binding sites overlap and that any genes sharing common binding sites are predominantly associated with lipid metabolism (55). To determine any possible SREBP subtype specificity in the low cholesterol-mediated transcriptional up-regulation of the hIP, the effect of ectopic expression of constitutively active SREBP1a and SREBP2, encoding their bHLH-LZ domains, was investigated. In all cell types, over-expression of SREBP1a^{-460}, but not SREBP2^{-468}, led to substantial increases in hIP mRNA levels and PrmIP-directed luciferase activity strongly suggesting an SREBP1-specific mechanism. Moreover, inhibition of SREBP activation using a PI3K inhibitor greatly abrogated the effects of reduced serum cholesterol on agonist-induced cAMP generation. These data are fully consistent with previous studies showing SREBP1, but not SREBP2, -dependent transactivation of the LDLR and COX2 promoters and with the fact that SREBP1 is the predominant form expressed in endothelial cells (39,59). While RT-PCR analyses suggested that SREBP1a, as opposed to SREBP1c, is the predominant SREBP1 member expressed in the vascular endothelial and megakaryocytic cells investigated herein, the studies do not exclude a possible role for SREBP1c in regulating IP expression in other cell or, more likely, tissue types where it is highly regulated and known to play a more predominant role (43,60).

SREBPs often cooperate with other DNA-binding proteins to achieve maximal transcriptional activation. For example, NF-Y and CREB cooperate with SREBP1 to regulate the HMG-CoA reductase gene whereas SREBP1 cooperates with Sp1 to activate the LDL receptor gene (50,61,62). Furthermore, SREBP1 and Sp1 have been identified as the two major transcription activators of the fatty acid synthase gene (*FASN*), one of the key enzymes in fatty acid synthesis (63). Critically, regulation by these additional *trans*-acting factors permits modulation of SREBP's transcriptional activity independently of its sterol-regulated proteolytic processing (**Figure 6A**). In addition to the functional SRE identified herein, a previously described Sp1 element lies in close proximity within the core promoter region of PrmIP that is essential for basal hIP gene expression (40). As stated, mutational disruption of the SRE alone significantly impaired the low cholesterol-inductions of PrmIP-directed gene expression. Interestingly, mutation of both the SRE and Sp1 *cis*-elements were necessary to completely abrogate the low-cholesterol induction suggesting a role for Sp1 in regulating PrmIP in response to cholesterol levels in addition to its established role within the core promoter in regulating basal hIP expression (40). Moreover, ChIP analysis confirmed that both endogenous Sp1 and SREBP1 bind *in vivo* to chromatin in close proximity to each other within the core region of PrmIP. While the levels of Sp1 expression and binding were unchanged in response to altered cholesterol levels, SREBP1 occupancy did not occur in high cholesterol but increased substantially following its depletion in low cholesterol serum. These findings most likely reflect the elevated levels of the proteolytically cleaved, 'transcriptionally-active' SREBP1 available for binding in low cholesterol conditions. Collectively, these data provide evidence of a coordinated role between SREBP1 and Sp1 in mediating the cholesterol-regulation of hIP gene expression.

As stated, recent studies have established central roles for Sp1, PU.1, Oct-1 and C/EBPδ in the transcriptional regulation of the hIP gene (**Figure 6B**; (40,41)). In an additional study, an evolutionary conserved ERE was also located within an upstream region of the human PrmIP that was found to be critical for regulation of the hIP in response to estrogen (**Figure 6B**;(32)). Herein, we have identified an evolutionary conserved *cis*-acting SRE critical for the transcriptional regulation of the hIP in model and primary cell lineages derived from the human vasculature and confirmed that the hIP gene is regulated by cholesterol-depletion through a direct SREBP1-SRE-dependent transcriptional mechanism, with a possible coordinate role, *albeit* minor, for Sp1. Collectively, these cell-based studies provide an important molecular and genetic platform for understanding the critical role of the hIP as a potential mediator, at least in part, of the effects of estrogen (32) but also of reduced cholesterol levels to the mechanisms of cardio-protection. The data also provides additional critical insights into the transcriptional regulation of the IP gene and for understanding the many diverse functions of prostacyclin and the hIP and may possibly explain, at least in part, some of pleiotropic beneficial effects of cholesterol-lowering agents within the vasculature. Furthermore, in addition to the proposed endothelial benefits, the fact that the hIP is also up-regulated by low cholesterol in the platelet progenitor megakaryocytic HEL cell line, *albeit* to a lesser extent than in either endothelial cell type investigated herein, clearly suggests that low cholesterol levels, or indeed cholesterol-lowering agents, may also elevate IP expression in platelets and, thereby, may confer added *anti*-thrombotic benefits in addition to the endothelial benefits, such as in reducing the risk of coronary artery disease.

Materials & Methods

Materials: pGL3Basic, pRL-Thymidine Kinase (pRL-TK), and Dual Luciferase® Reporter Assay System were obtained from Promega Corporation and pCRE-Luc from Strategene. DMRIE-C® was from Invitrogen Life Technologies and Effectene® from Qiagen. *Anti*-Sp1 (sc-59x), *anti*-SREBP1 (sc-366x), normal rabbit IgG (sc-2027) and goat *anti*-rabbit horseradish peroxidise (sc-2204) were obtained from Santa Cruz Biotechnology. *Anti*-HDJ-2 antibody and *anti*-FLAG-HRP-conjugated M2 antibody were from Neomarkers. Cholesterol, 25-hydroxycholesterol, actinomycinD (ActD), cycloheximide (CHX) and Ly294002 (Ly) were from Sigma. Delipidated fetal bovine serum (FBS) was from PanBiotech, Germany.

Cell Culture

Human erythroleukemic (HEL) 92.1.7 cells (64), obtained from the American Type Culture Collection, were cultured in RPMI 1640, 10 % FBS. Human endothelial EA.hy926 cells (56), obtained from the Tissue Culture Facility at UNC Lineberger Comprehensive Cancer Centre, Chapel Hill, NC, were cultured in DMEM, 10 % FBS. Primary (1°) human umbilical vein endothelial cells (HUVECs) were purchased Lonza (IRT9-048-0904D) and cultured in M199 media supplemented with 0.4 % (v/v) Endothelial Cell Growth Supplement/Herparin (ECGS/H; Lonza), 10% FBS. As necessary, in order to modify cholesterol levels in the cell culture media, cells were serum starved overnight and then subsequently cultured for 24 h in either normal serum (NS; 10 % FBS), low cholesterol serum (LCS; 10 % delipidated FBS) or high cholesterol serum (HCS; 10 % FBS, 10 µg/ml cholesterol and 1 µg/ml 25-hydroxycholesterol), respectively, essentially as previously described (39). All mammalian cells were grown at 37 ^{o}C in a humid environment with 5 % CO_2 and were confirmed to be free of mycoplasma contamination.

Luciferase-based Genetic Reporter Plasmids

The plasmid pGL3B:PrmIP, encoding PrmIP (-2449 to -772, relative to the translation start codon at +1) from the human prostacyclin receptor (IP) in the pGL3Basic reporter vector, in addition to pGL3B:PrmIP1, pGL3B:PrmIP2, pGL3B:PrmIP3, pGL3B:PrmIP4, pGL3B:PrmIP5, pGL3B:PrmIP6, pGL3B:PrmIP6^{Sp1*}, pGL3B:PrmIP6$^{PU.1*}$, pGL3B:PrmIP6$^{Oct\text{-}1*}$ and pGL3B:PrmIP7 were previously described (40). Site-directed mutagenesis of the SRE (-937) from tgcTCACcc to tgc**C**CACcc was carried by Quik-Change^{TM} method (Stratagene) using pGL3B:PrmIP6 or pGL3B:PrmIP6^{Sp1*} as template and primers Kin784 (5'-d GAAATGAAAAAGCTGGGGTG**G**GCAGGCAAGCTGAGGAGG -3') and complementary Kin785 to generate pGL3B:PrmIP6^{SRE*} or pGL3B:$^{PrmIP6Sp1*/SRE*}$ respectively. The fidelity of all plasmids was confirmed by DNA sequence analysis.

Real-time PCR Analysis

Total RNA was isolated using TRIzol reagent (Invitrogen Life Technologies) from 1^{o} HUVECs, HEL 92.1.7 and EA.hy926 cells that had been serum-starved overnight and then cultured for 24 h in either NS, LCS or HCS and/or ActD (10 µg/ml) or CHX (20 µg/ml) as indicated. DNase 1-treated total RNA was converted to first strand (1^{o}) cDNA with MMLV RT (Promega). For semi-quantitative RT-PCR, primers were designed to specifically amplify hIP mRNA sequences (5'-dGAAGGCACAGACGCACGGGA -3', Nu -57 to -37; Kin264) and (5'-dGGCGAAGGCGAAGGCATCGC -3'; Nu 294 to 275; Kin266) or, as an internal control, to amplify glyceraldehyde-3-phosphate dehydrogenase (GA3'PDH) mRNA (5'-dTGAAGGTCGGAGTCAACG-3'; Nu 527-545; Kin291) and (5'-dCATGTGGGCCATGAGGTC-3'; Nu 993-976; DT92). All primers were designed to span across an intron such that only PCR products from 1^{o} cDNA would be amplified, thereby eliminating genomic artifacts.

Alternatively, real-time quantitative (QT) -PCR analysis was performed using the Brilliant II SYBR® Green QPCR master mix system (Agilent; #600828) and spectrofluorometric thermal cycler (Agilent) with primers designed to specifically amplify hIP mRNA sequences (forward, 5'-GAAGGCACAGACGCACGGGA-3', Nu -57 to -37 of Exon 1; Kin264 and reverse 5'-GGCGAAGGCGAAGGCATCGC -3'; Nu 294 to 275 of Exon 2; Kin266; 348 bp amplicon), SREBP1a mRNA sequences (forward, 5'-TCAGCGAGGCGGCTTTGGAGCAG-3'; Kin1289 and

reverse 5'-CATGTCTTCGATGTCGGTCAG-3'; Kin1290; 85 bp amplicon), SREBP1c mRNA sequences (forward, 5'-GGAGGGGTAGGGCCAACGGCCT-3'; Kin1291 and reverse 5'-CATGTCTTCGAAAGTGCAATCC-3'; Kin1292; 80 bp amplicon), or, as an internal control, using primers designed to amplify a 588 bp region of the human 18s rRNA gene (forward, 5'-CGGCTACCACATCCAAGGAA-3'; reverse, 5'-TCGTCTTCGAACCTCCGACT-3'). The levels of hIP, SREBP1a and SREBP1c mRNA were normalized using corresponding 18s rRNA expression levels, to obtain Ct values. Relative IP mRNA expression levels were then calculated using the formula $2^{-\Delta\Delta Ct}$ (65). Data is presented as either relative levels of mRNA expression or as mean changes in mRNA expression in cells cultured in LCS or HCS relative to those levels in control transfected (pCMV7) or NS culture conditioned cells, set to a value of 1 (Relative expression ± SEM, n = 3).

Assay of Luciferase Activity

HEL 92.1.7 and EA.hy926 cells were co-transfected with various pGL3Basic-recombinant plasmids, encoding firefly luciferase, along with pRL-TK, encoding renilla luciferase, using DMRIE-C® transfection reagent as previously described (40). In the case of the 1° HUVECs, in brief, 24 h prior to transfection cells were plated in 6-well format to achieve 60-80 % confluency at time of transfection and were co-transfected with recombinant pGL3Basic-recombinant plasmids (2 μg) and pRL-TK (200 ng) using 5 μl Effectene® reagent as per the manufacturer's instructions (Qiagen). In all cell types, cells were serum-starved overnight and then the media was changed 24 h post-transfection to either NS, LCS or HCS, as indicated. Firefly and renilla luciferase activity was assayed 24 h later (48 h post-transfection) using the Dual Luciferase Assay System®. To investigate the effect of over-expression of constitutively active forms of SREBP1a and SREBP2 on PrmIP6-directed luciferase expression, pCMV7 recombinant plasmids encoding FLAG-tagged forms of SREBP1a^{-460} or SREBP2^{-468} (0-2.0 μg; ATCC) or, as a negative control, pCMV7, were transiently transfected into HEL, EA.hy926 or 1° HUVECs, as described above, along with recombinant pGL3B:PrmIP6. Firefly and renilla luciferase activity was assayed after 48 h using the Dual Luciferase Assay System®. Relative firefly to renilla luciferase activities (arbitrary units) were calculated as a ratio and were expressed in relative luciferase units (RLU).

A gene reporter assay system based on use of cAMP-responsive promoter containing a CRE (cAMP-response element) was performed to investigate agonist-induced changes in the intracellular cAMP levels, essentially as described (32). In brief, the luciferase reporter plasmid pCRE-Luc (1 μg; Stratagene) was co-transfected with 50 ng pRL-TK into 1° HUVECs, EA.hy926 and HEL cells. In all cell types, cells were serum-starved overnight and then the media was changed 24 h post-transfection to either NS, LCS or HCS and cultured for a further 24 hr. Where indicated, cells were incubated with either vehicle (V; PBS, 0.01% EtOH) or Ly294002 (20 μM) for 24 h. Thereafter, at 48 h post-transfection, cells were treated with 3-isobutyl-1-methylxanthine (IBMX; 100 μM) at 37 °C for 30 min and then stimulated with either vehicle (V; DMSO) or 1 μM cicaprost at 37 °C for 3 h. Firefly and renilla luciferase activity was assayed 52 hr post-transfection using the Dual Luciferase Assay System® and cAMP levels generated in vehicle- or cicaprost-treated cells were measured expressed as a ratio (relative luciferase units; RLU) or as fold-inductions in cAMP accumulation.

Western Blot Analysis

Both ectopic expression of the constitutively active SREBP proteins, e.g encoded by pCMV7:SREBP1a^{-460} or pCMV7:SREBP2^{-468}, and endogenous expression of Sp1 and SREBP1 in HEL, EA.hy926 and 1° HUVECs was confirmed by western blot analysis. Briefly, whole cell protein was resolved by SDS-PAGE (10 % acrylamide gels) and transferred to polyvinylidene difluoride (PVDF) membrane according to standard methodology. Membranes were screened using either *anti*-FLAG, *anti*- Sp1 and *anti*- SREBP1 sera in 5 % non-fat dried milk in 1 x TBS (0.01 M Tris-HCl, 0.1 M NaCl, pH 7.4) for 2 h at room temperature followed by washing and screening using goat *anti*-rabbit horseradish peroxidase followed by chemiluminescence detection. To confirm uniform protein loading, the blots were stripped and rescreened with *anti*-HDJ-2 antibody (Neomarkers) to detect endogenous HDJ-2 protein expression. In all cases the relative levels of Sp1/SREBP1 expression in

NS, LCS or HCS-cultured cells were normalized relative to that of the ubiquitously expressed chaperone protein HDJ-2, which served as a general protein loading control.

ChIP analysis

Chromatin immunoprecipitation (ChIP) assays were performed as previously described (40). Briefly, cells (1 x 10^8) were grown to 70 % confluency, serum starved overnight and subsequently cultured for 24 h in either NS, LCS or HCS, as indicated. Cells were then collected by centrifugation at 2,000 g for 5 min at 4 ^oC, washed twice in ice-cold PBS and resuspended in 50 ml serum-free RPMI. Formaldehyde (1 %)-cross linked chromatin was sonicated to generate fragments 500 bp to 1000 bp in length and sheared chromatin was resuspended in a final volume of 6 ml Lysis Buffer (40). Prior to immunoprecipitation, chromatin was incubated with 60 µg normal rabbit IgG overnight at 4 ^oC on a rotisserie, after which 250 µl of salmon sperm DNA/protein A agarose beads (Millipore) were added and chromatin was precleared overnight at 4 ^oC with rotation. Thereafter, for ChIP assays, aliquots (672 µl) of the precleared chromatin were incubated with either *anti*-SREBP1, *anti*-Sp1 (10 µg aliquots) or, as a control, normal rabbit IgG (10 µg) antibodies or in the absence of primary (1^o) antibody (-AB). Precleared chromatin aliquots (270 µl) were stored for use as inputs. All antibodies used for ChIP analysis were ChIP-validated by the supplier (Santa Cruz) and have been used previously for such analyses (66,67). Following elution of the immune complexes from the Protein A Agarose/Salmon sperm DNA (Millipore #16-157C), cross-links were reversed by incubation at 65 ^oC overnight followed by protease digestion with proteinase K (Gibco-BRL #25530-031; 9 µl of 10 mg/ml) at 45 ^oC for 5 h. After precipitation, samples were resuspended in 50 µl dH_2O. PCR analysis was carried out using 2-3 µl of ChIP sample as template or, as a positive control, with an equivalent volume of a 1:20 dilution of the input chromatin DNA. Sequences of the primers used for the ChIP PCR reactions and corresponding nucleotides within PrmIP or the LDL receptor promoter include;

1. Kin538, 5′-dGAGA GGTACC ACCCTGAGACAGCCCAGG-3′, Nu -1271 to -1243
2. Kin274, 5′-dCTCTCAAGCTTCTCTCCAGTCTTGCCCAGGCTC -3′ , Nu -807 to -774
3. Kin676, 5′-dGAGAGGTACCCAGAGAGGGTCTCTG -3′ , Nu -1901 to -1886
4. Kin677, 5′-dCTCTAAGCTTGGAGACTTCCATGGC -3′ , Nu -1555 to -1540
5. Kin1295, 5′-d CGATGTCACATCGGCCGTTCG -3′ , Nu -124 to -103 (68)
6. Kin1296, 5′-d CACGACCTGCTGTGTCCTAGCTGGAA -3′ , Nu +29 to +55 (68)

Alternatively, for quantitation of the relative abundance of the PCR products derived from the individual test or control immunoprecipitates relative to that of the products derived from the respective input chromatins, real-time QT-PCR reactions were carried out for the same number of cycles (typically 35 cycles) using the Agilent MX3005P QPCR system to obtain cycle threshold (Ct) values. Changes in relative PCR product intensities were then calculated using the Relative Quantification method using the formula $2^{-\Delta\Delta Ct}$ (65). Data is presented as mean product intensities of the individual test or control immunoprecipitates expressed as a percentage relative to those derived from the corresponding input chromatins. For all ChIP-based experiments, PCR (semi-quantitative and real time QT-PCR) data presented is obtained from at least 3 independent ChIP immunoprecipitations using chromatin extracted on at least 3 occasions, rather than from triplicate PCRs using chromatin precipitated from single ChIP experiments.

Immunofluorescence Microscopy

To examine hIP expression, 1^o HUVECs were grown on poly-L-lysine treated coverslips, in 6-well plates. Cells were then serum starved overnight and subsequently cultured for 24 h in either (i) HCS, (ii) NS, (iii) NS:LCS (3:1); 7.5 % NS and 2.5 % LCS, (iv) NS:LCS (1:1); 5 % NS and 5 % LCS or (v) LCS. Thereafter, cells were fixed using 3.7 % paraformaldehyde in PBS pH 7.4 for 15 min at RT prior to washing in PBS. Cells were permeabilized by incubation with 0.2 % Triton X-100 in PBS for 10 min on ice, followed by washing in TBS. Non-specific sites were blocked by incubating cells with 1 % BSA in TBS, pH 7.4 for 1 h at RT. Cells were incubated with the affinity purified rabbit polyclonal *anti*-hIP antibody (1 : 500; 1 % BSA in TBS)(32) to label the hIP for 1 h at RT. As additional controls, the *anti*-hIP antibody was pre-incubated with its cognate antigenic peptide, corresponding to intracellular loop $(IC)_2$ of the hIP, (10 µg/ml) prior to exposure to cells in LCS

media. The primary antibody solution was removed and cells were washed with TBS followed by a further incubation with 1 % BSA in TBS-T for 30 min. Cells were then incubated with AlexaFluor488 goat *anti*-rabbit IgG secondary antibody (1 : 2000; 1 % BSA in TBS-T) for 1 h at RT to detect the IP receptor. After washing, all slides were counterstained with 4′,6-diamidino-2-phenylindole (DAPI, 1 µg/ml in H_2O) prior to mounting coverslips in DakoCytomation fluorescence mounting medium. Imaging was carried out using the Zeiss Axioplan 2 microscope and Axioplan Version 4.4 imaging software. Data presented are representative images for at least three independent experiments from which at least 10 fields were viewed at 63X magnification, where the horizontal bar represents 10 µM. Endogenous hIP expression was analysed and normalized against DAPI nuclear staining using ImageJ software integrated density analysis and data is presented as mean changes in hIP expression in cells cultured in LCS, NS:LCS (3:1 and 1:1) or HCS relative to those levels in NS culture conditioned cells, set to a value of 100 % (Relative expression ± SEM, n = 3).

Statistical Analysis

Statistical analyses of differences were carried out using the unpaired Student's ***t*** test or one-way ANOVA followed by post hoc Dunnett's multiple comparison ***t*** tests, employing GraphPad Prism, version 4.00 package. All values are expressed as mean ± standard error of the mean (SEM). *P*-values ≤ 0.05 were considered to indicate statistically significant differences and, as relevant, *, **, *** and **** indicate $p \leq 0.05$, 0.01, 0.001 and 0.0001, respectively.

References

1. Gryglewski, R. J. (2008) *Pharmacol Rep* **60**, 3-11
2. Narumiya, S., Sugimoto, Y., and Ushikubi, F. (1999) *Physiological reviews* **79**, 1193-1226
3. Kawabe, J., Ushikubi, F., and Hasebe, N. (2010) *Circulation journal : official journal of the Japanese Circulation Society* **74**, 836-843
4. Hayes, J. S., Lawler, O. A., Walsh, M. T., and Kinsella, B. T. (1999) *The Journal of biological chemistry* **274**, 23707-23718
5. Miggin, S. M., Lawler, O. A., and Kinsella, B. T. (2003) *The Journal of biological chemistry* **278**, 6947-6958
6. O'Keeffe, M. B., Reid, H. M., and Kinsella, B. T. (2008) *Biochimica et biophysica acta* **1783**, 1914-1928
7. Reid, H. M., Mulvaney, E. P., Turner, E. C., and Kinsella, B. T. (2010) *The Journal of biological chemistry* **285**, 18709-18726
8. Turner, E. C., Mulvaney, E. P., Reid, H. M., and Kinsella, B. T. (2011) *Mol Biol Cell* **22**, 2664-2679
9. Wikstrom, K., Reid, H. M., Hill, M., English, K. A., O'Keeffe, M. B., Kimbembe, C. C., and Kinsella, B. T. (2008) *Cellular signalling* **20**, 2332-2346
10. Wilson, S. J., and Smyth, E. M. (2006) *The Journal of biological chemistry* **281**, 11780-11786
11. Fitzgerald, D. J., Entman, S. S., Mulloy, K., and FitzGerald, G. A. (1987) *Circulation* **75**, 956-963
12. Kahn, N. N., Mueller, H. S., and Sinha, A. K. (1990) *Circ Res* **66**, 932-940
13. Komhoff, M., Lesener, B., Nakao, K., Seyberth, H. W., and Nusing, R. M. (1998) *Kidney Int* **54**, 1899-1908
14. Gomberg-Maitland, M., and Olschewski, H. (2008) *Eur Respir J* **31**, 891-901
15. Fetalvero, K. M., Martin, K. A., and Hwa, J. (2007) *Prostaglandins & other lipid mediators* **82**, 109-118
16. Sakai, A., Yajima, M., and Nishio, S. (1990) *Life Sci* **47**, 711-719
17. Xiao, C. Y., Hara, A., Yuhki, K., Fujino, T., Ma, H., Okada, Y., Takahata, O., Yamada, T., Murata, T., Narumiya, S., and Ushikubi, F. (2001) *Circulation* **104**, 2210-2215
18. Zachary, I. (2001) *Am J Physiol Cell Physiol* **280**, C1375-1386
19. Patrignani, P., Di Febbo, C., Tacconelli, S., Douville, K., Guglielmi, M. D., Horvath, R. J., Ding, M., Sierra, K., Stitham, J., Gleim, S., Baccante, G., Moretta, V., Di Francesco, L., Capone, M. L., Porreca, E., and Hwa, J. (2008) *Pharmacogenetics and genomics* **18**, 611-620

20. Stitham, J., Arehart, E. J., Gleim, S., Douville, K., MacKenzie, T., and Hwa, J. (2007) *Gene* **396**, 180-187
21. Stitham, J., Stojanovic, A., and Hwa, J. (2002) *The Journal of biological chemistry* **277**, 15439-15444
22. Arehart, E., Stitham, J., Asselbergs, F. W., Douville, K., MacKenzie, T., Fetalvero, K. M., Gleim, S., Kasza, Z., Rao, Y., Martel, L., Segel, S., Robb, J., Kaplan, A., Simons, M., Powell, R. J., Moore, J. H., Rimm, E. B., Martin, K. A., and Hwa, J. (2008) *Circulation research* **102**, 986-993
23. Stitham, J., Arehart, E., Elderon, L., Gleim, S. R., Douville, K., Kasza, Z., Fetalvero, K., MacKenzie, T., Robb, J., Martin, K. A., and Hwa, J. (2011) *The Journal of biological chemistry* **286**, 7060-7069
24. Bley, K. R., Hunter, J. C., Eglen, R. M., and Smith, J. A. (1998) *Trends Pharmacol Sci* **19**, 141-147
25. Hoshikawa, Y., Voelkel, N. F., Gesell, T. L., Moore, M. D., Morris, K. G., Alger, L. A., Narumiya, S., and Geraci, M. W. (2001) *Am J Respir Crit Care Med* **164**, 314-318
26. Murata, T., Ushikubi, F., Matsuoka, T., Hirata, M., Yamasaki, A., Sugimoto, Y., Ichikawa, A., Aze, Y., Tanaka, T., Yoshida, N., Ueno, A., Oh-ishi, S., and Narumiya, S. (1997) *Nature* **388**, 678-682
27. Stitham, J., Arehart, E. J., Gleim, S. R., Douville, K. L., and Hwa, J. (2007) *Prostaglandins & other lipid mediators* **82**, 95-108
28. Sugimoto, Y., Narumiya, S., and Ichikawa, A. (2000) *Progress in lipid research* **39**, 289-314
29. Kawabe, J., Yuhki, K., Okada, M., Kanno, T., Yamauchi, A., Tashiro, N., Sasaki, T., Okumura, S., Nakagawa, N., Aburakawa, Y., Takehara, N., Fujino, T., Hasebe, N., Narumiya, S., and Ushikubi, F. (2010) *Arteriosclerosis, thrombosis, and vascular biology* **30**, 464-470
30. Egan, K. M., Lawson, J. A., Fries, S., Koller, B., Rader, D. J., Smyth, E. M., and Fitzgerald, G. A. (2004) *Science* **306**, 1954-1957
31. Ospina, J. A., Krause, D. N., and Duckles, S. P. (2002) *Stroke* **33**, 600-605
32. Turner, E. C., and Kinsella, B. T. (2010) *J Mol Biol* **396**, 473-486 (Corrigendum, J Mol Biol (2011), 2413, 2899)
33. Vogel, R. A. (1999) *The American journal of medicine* **107**, 479-487
34. Corsini, A., Bellosta, S., Baetta, R., Fumagalli, R., Paoletti, R., and Bernini, F. (1999) *Pharmacol Ther* **84**, 413-428
35. Guijarro, C., Blanco-Colio, L. M., Ortego, M., Alonso, C., Ortiz, A., Plaza, J. J., Diaz, C., Hernandez, G., and Egido, J. (1998) *Circulation research* **83**, 490-500
36. Laufs, U., and Liao, J. K. (2000) *Trends Cardiovasc Med* **10**, 143-148
37. Arnaud, C., Veillard, N. R., and Mach, F. (2005) *Curr Drug Targets Cardiovasc Haematol Disord* **5**, 127-134
38. Smith, L. H., Boutaud, O., Breyer, M., Morrow, J. D., Oates, J. A., and Vaughan, D. E. (2002) *Arteriosclerosis, thrombosis, and vascular biology* **22**, 983-988
39. Smith, L. H., Petrie, M. S., Morrow, J. D., Oates, J. A., and Vaughan, D. E. (2005) *Journal of lipid research* **46**, 862-871
40. Turner, E. C., and Kinsella, B. T. (2009) *J Mol Biol* **386**, 579-597
41. Keating, G., Turner, E. C., and Kinsella, B. T. (2012) *Biochimica et biophysica acta* **1819**, 428-445
42. Quandt, K., Frech, K., Karas, H., Wingender, E., and Werner, T. (1995) *Nucleic Acids Res* **23**, 4878-4884
43. Bengoechea-Alonso, M. T., and Ericsson, J. (2007) *Current opinion in cell biology* **19**, 215-222
44. Eberle, D., Hegarty, B., Bossard, P., Ferre, P., and Foufelle, F. (2004) *Biochimie* **86**, 839-848
45. Horton, J. D., Goldstein, J. L., and Brown, M. S. (2002) *The Journal of clinical investigation* **109**, 1125-1131
46. Horton, J. D., Shah, N. A., Warrington, J. A., Anderson, N. N., Park, S. W., Brown, M. S., and Goldstein, J. L. (2003) *Proc Natl Acad Sci U S A* **100**, 12027-12032
47. Osborne, T. F., and Espenshade, P. J. (2009) *Genes & development* **23**, 2578-2591

48. Jeon, T. I., and Osborne, T. F. (2012) *Trends in endocrinology and metabolism: TEM* **23**, 65-72
49. Shimomura, I., Shimano, H., Korn, B. S., Bashmakov, Y., and Horton, J. D. (1998) *The Journal of biological chemistry* **273**, 35299-35306
50. Sanchez, H. B., Yieh, L., and Osborne, T. F. (1995) *The Journal of biological chemistry* **270**, 1161-1169
51. Krycer, J. R., Sharpe, L. J., Luu, W., and Brown, A. J. (2010) *Trends in endocrinology and metabolism: TEM* **21**, 268-276
52. Du, X., Kristiana, I., Wong, J., and Brown, A. J. (2006) *Mol Biol Cell* **17**, 2735-2745
53. Tyroler, H. A. (1985) *American journal of preventive medicine* **1**, 18-24
54. Hadi, H. A., Carr, C. S., and Al Suwaidi, J. (2005) *Vascular health and risk management* **1**, 183-198
55. Seo, Y. K., Jeon, T. I., Chong, H. K., Biesinger, J., Xie, X., and Osborne, T. F. (2011) *Cell metabolism* **13**, 367-375
56. Suggs, J. E., Madden, M. C., Friedman, M., and Edgell, C. J. (1986) *Blood* **68**, 825-829
57. Dawson, P. A., Hofmann, S. L., van der Westhuyzen, D. R., Sudhof, T. C., Brown, M. S., and Goldstein, J. L. (1988) *The Journal of biological chemistry* **263**, 3372-3379
58. Briggs, M. R., Yokoyama, C., Wang, X., Brown, M. S., and Goldstein, J. L. (1993) *The Journal of biological chemistry* **268**, 14490-14496
59. Yokoyama, C., Wang, X., Briggs, M. R., Admon, A., Wu, J., Hua, X., Goldstein, J. L., and Brown, M. S. (1993) *Cell* **75**, 187-197
60. Amemiya-Kudo, M., Shimano, H., Hasty, A. H., Yahagi, N., Yoshikawa, T., Matsuzaka, T., Okazaki, H., Tamura, Y., Iizuka, Y., Ohashi, K., Osuga, J., Harada, K., Gotoda, T., Sato, R., Kimura, S., Ishibashi, S., and Yamada, N. (2002) *Journal of lipid research* **43**, 1220-1235
61. Smith, J. R., Osborne, T. F., Brown, M. S., Goldstein, J. L., and Gil, G. (1988) *The Journal of biological chemistry* **263**, 18480-18487
62. Edwards, P. A., Tabor, D., Kast, H. R., and Venkateswaran, A. (2000) *Biochimica et biophysica acta* **1529**, 103-113
63. Jeon, B. N., Kim, Y. S., Choi, W. I., Koh, D. I., Kim, M. K., Yoon, J. H., Kim, M. Y., Hur, B., Paik, P. D., and Hur, M. W. (2012) *Journal of lipid research* **54**, 755-766
64. Long, M. W., Heffner, C. H., Williams, J. L., Peters, C., and Prochownik, E. V. (1990) *The Journal of clinical investigation* **85**, 1072-1084
65. Livak, K. J., and Schmittgen, T. D. (2001) *Methods* **25**, 402-408
66. Liu, S., Luo, H., Liu, J., McNeilly, A. S., and Cui, S. (2008) *Biochemical and biophysical research communications* **366**, 36-41
67. Schroeder-Gloeckler, J. M., Rahman, S. M., Janssen, R. C., Qiao, L., Shao, J., Roper, M., Fischer, S. J., Lowe, E., Orlicky, D. J., McManaman, J. L., Palmer, C., Gitomer, W. L., Huang, W., O'Doherty, R. M., Becker, T. C., Klemm, D. J., Jensen, D. R., Pulawa, L. K., Eckel, R. H., and Friedman, J. E. (2007) *The Journal of biological chemistry* **282**, 15717-15729
68. Smith, J. R., Osborne, T. F., Goldstein, J. L., and Brown, M. S. (1990) *The Journal of biological chemistry* **265**, 2306-2310
69. Guan, G., Dai, P. H., Osborne, T. F., Kim, J. B., and Shechter, I. (1997) *The Journal of biological chemistry* **272**, 10295-10302
70. Sato, R., Inoue, J., Kawabe, Y., Kodama, T., Takano, T., and Maeda, M. (1996) *The Journal of biological chemistry* **271**, 26461-26464

Figure 1

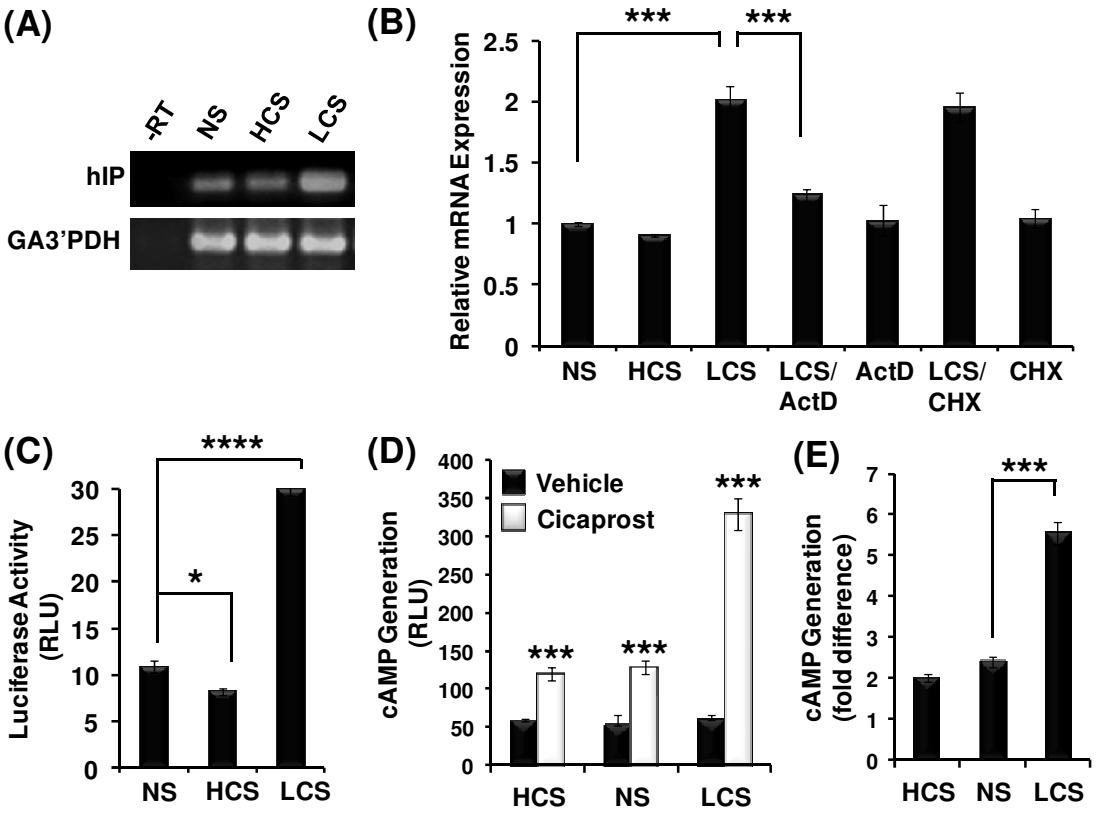

Figure 1: **Effect of cholesterol on hIP mRNA, PrmIP-directed gene expression and hIP-induced cAMP generation in EA.hy926 cells.**
RT-PCR (**Panel A**) and real-time quantitative RT-PCR (**Panel B**) analysis of hIP and GA3'PDH mRNA expression in EA.hy926 cells cultured for 24 h in either normal serum (NS; 10 % FBS), high cholesterol serum (HCS; 10 % FBS, 10 μg/ml cholesterol and 1 μg/ml 25-hydroxycholesterol) or low cholesterol serum (LCS; 10 % delipidated FBS), in the absence or presence of ActD (10 μg/ml) or CHX (20 μg/ml) as indicated. **Panel C**: EA.hy926 cells were co-transfected with pGL3B:PrmIP plus pRL-TK; 24 h post-transfection media was replaced with NS, HCS or LCS and cells were cultured for an additional 24 h prior to measurement of PrmIP-directed luciferase reporter gene expression (RLU ± SEM; n = 6). Data is presented as mean firefly relative to renilla luciferase activity, expressed in arbitrary relative luciferase units (RLU ± SEM; n = 6). **Panels D & E**: EA.hy926 cells were co-transfected with pCRE-Luc; 24 h post-transfection, media was replaced with fresh NS, HCS or LCS media and cells were cultured for an additional 24 h. For measurement of agonist-induced cAMP generation, cells were stimulated for 3 h with cicaprost (1 μM) or, as controls, with the drug vehicle (V; PBS). Data is presented as hIP-induced cAMP accumulation (**Panel D**: RLU ± SEM, n =3) or as fold-inductions in cAMP accumulation in LCS relative to NS-cultured cells (**Panel E**). The asterisks (*) indicate where cholesterol depletion in LCS resulted in significant changes in either hIP mRNA, PrmIP-directed gene expression or hIP-induced cAMP generation relative to those levels in NS, where *, ***, and **** indicates $p < 0.05$, $p < 0.001$ and $p < 0.0001$, respectively, for post-hoc Dunnett's multiple comparison *t*-test analysis.

Figure 2

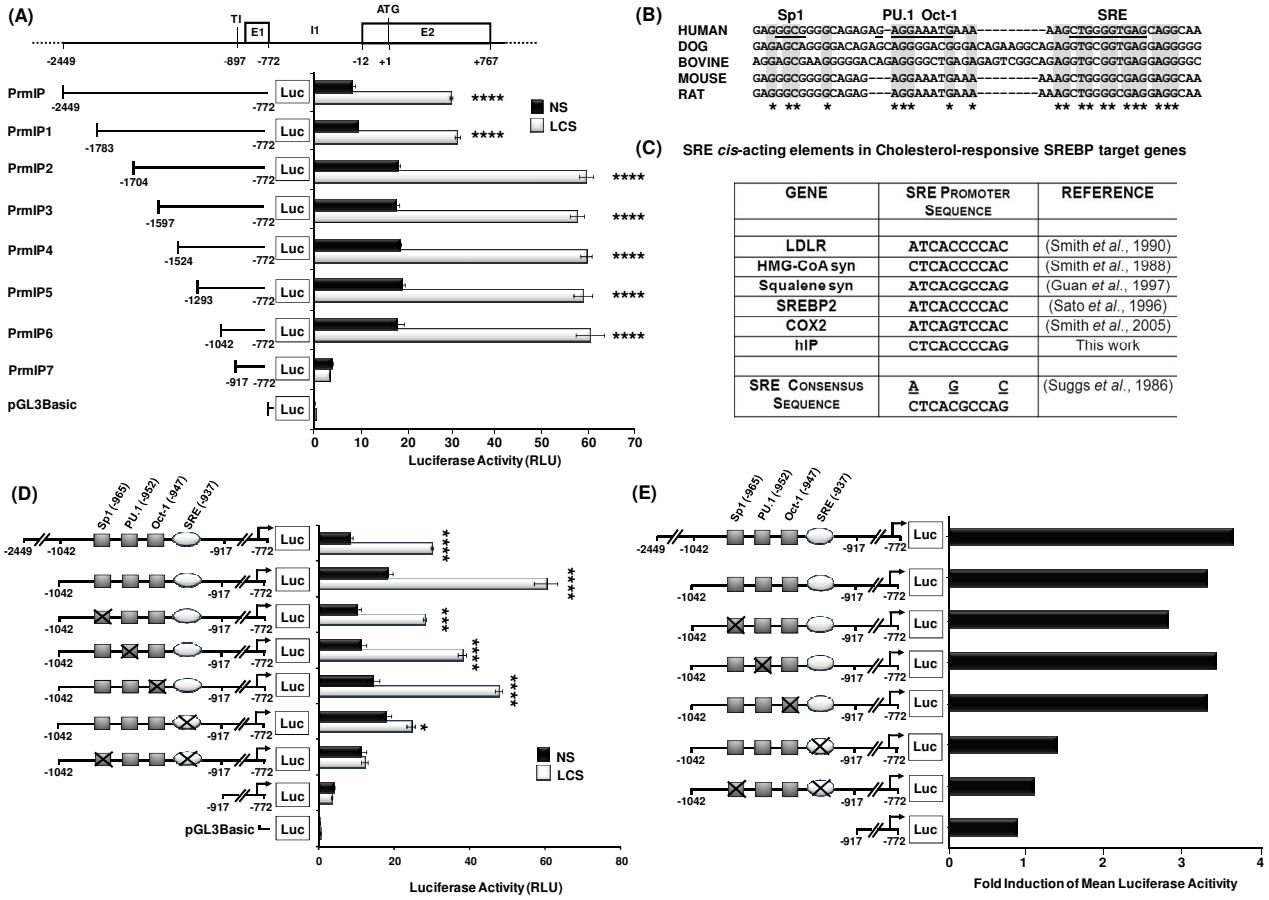

Figure 2: Identification of a putative SRE within PrmIP.
Panels A: Localisation of the cholesterol-responsive region within PrmIP by 5' deletion analysis. A schematic of the hIP genomic region, spanning nucleotides -2449 to +767, encoding PrmIP, exon (E)1, intron (I)1 and E2, where +1 corresponds to the translational start site. PrmIP-, PrmIP1-, PrmIP2-, PrmIP3-, PrmIP4-, PrmIP5-, PrmIP6- and PrmIP7-directed luciferase gene expression in EA.hy926 cells cultured for 24 h in NS or LCS (RLU ± SEM; n = 6). **Panel B:** Alignment of the basal and putative cholesterol-responsive region of human PrmIP with the IP promoter orthologue sequences from dog, bovine, mouse and rat. The Sp1, PU.1 and Oct-1 and the consensus SRE binding elements are underlined in the human PrmIP sequence while evolutionary conserved nucleotides are indicated by asterisks (*) and highlighted in grey in the orthologues. **Panel C:** SRE *cis*-acting elements in recognized cholesterol-responsive SREBP target genes (39,56,61,68-70). **Panels D & E:** A schematic of PrmIP6 in addition to the putative Sp1, PU.1, Oct-1 and SRE binding elements, where the 5' nucleotides are indicated in brackets (-965, -952, -947 and -937, respectively). PrmIP6, PrmIP6^{SP1*}, PrmIP6$^{PU.1*}$, PrmIP6$^{Oct\text{-}1*}$, PrmIP6^{SRE*}, PrmIP6$^{SRE/Sp1*}$ and PrmIP7-directed luciferase expression in EA.hy926 cells cultured for 24 h with either NS or LCS. Data in **Panels A & D** is presented as mean firefly relative to renilla luciferase activity expressed in arbitrary relative luciferase units (RLU ± SEM; n = 6) or in **Panel E** as fold-induction of mean luciferase activity in LCS- relative to that in NS- cultured cells. The asterisks (*) indicate where culturing cells in LCS led to significant increases in luciferase expression relative to that in NS, where *, ***, and **** indicates $p < 0.05$, $p < 0.001$ and $p < 0.0001$, respectively, for post-hoc Dunnett's multiple comparison *t*-test analysis.

Figure 3

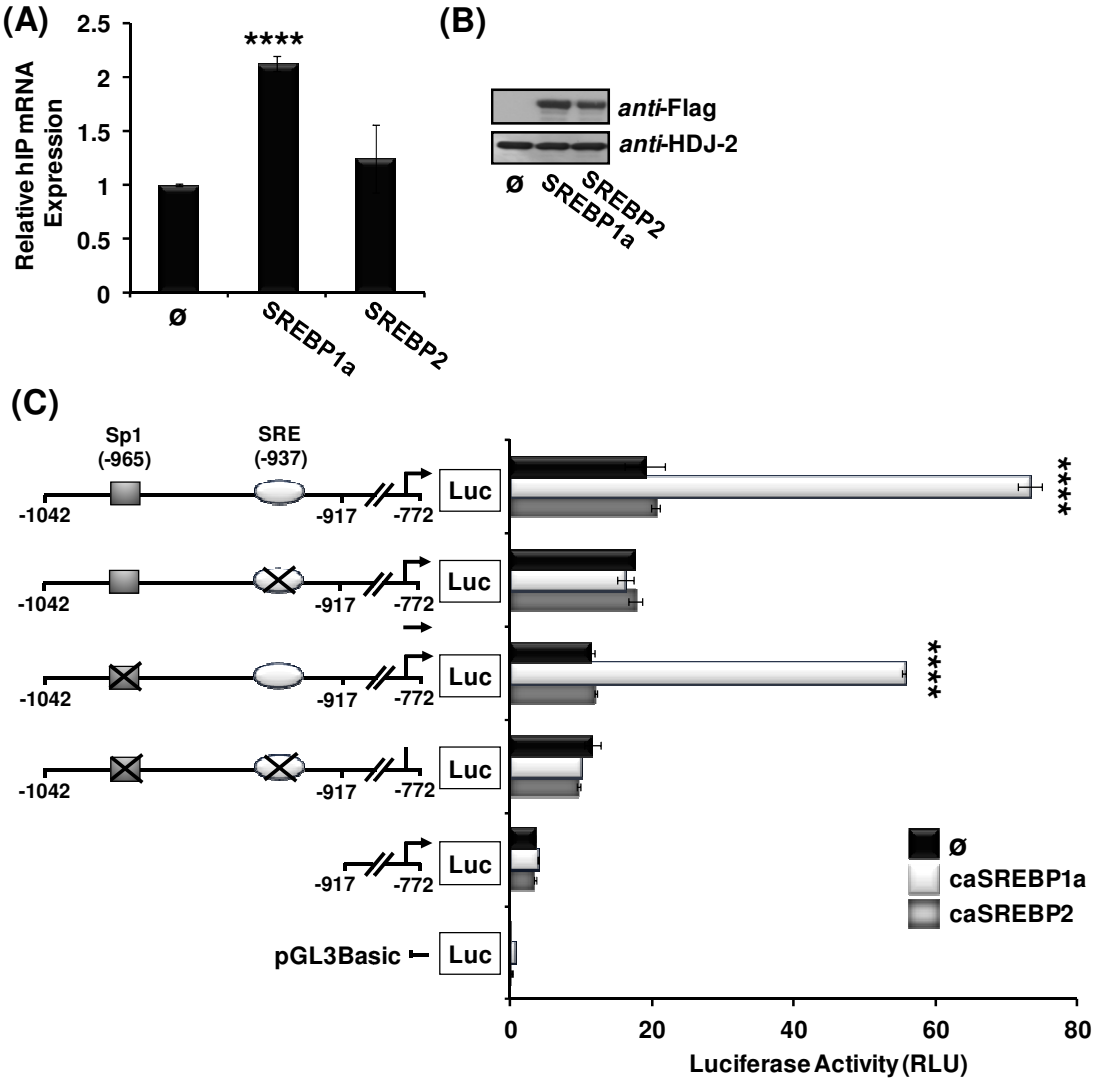

Figure 3: Effect of SREBP expression on hIP expression levels in EA.hy926 cells.
Panels A & C: Real-time quantitative RT-PCR analysis of the effect of ectopic expression of constitutively active SREBP1a^{-460} or SREBP2^{-468} on hIP relative to GA3'PDH mRNA expression (**Panel A**) and PrmIP-directed luciferase expression (**Panel C**) in EA.hy926 cells. The asterisks indicate where ectopic expression significantly increased either hIP mRNA levels or PrmIP-directed gene expression where **** indicates $p < 0.0001$, for post-hoc Dunnett's multiple comparison *t*-test analysis. **Panel B:** Immunoblot analysis of whole cell protein from EA.hy926 cells transfected with either the empty vector (ø) or with vectors encoding FLAG-tagged forms of SREBP1a^{-460} or SREBP2^{-468}, where blots were screened successively with *anti*-FLAG and *anti*-HDJ-2 antisera. Images are representative of three independent experiments.

Figure 4

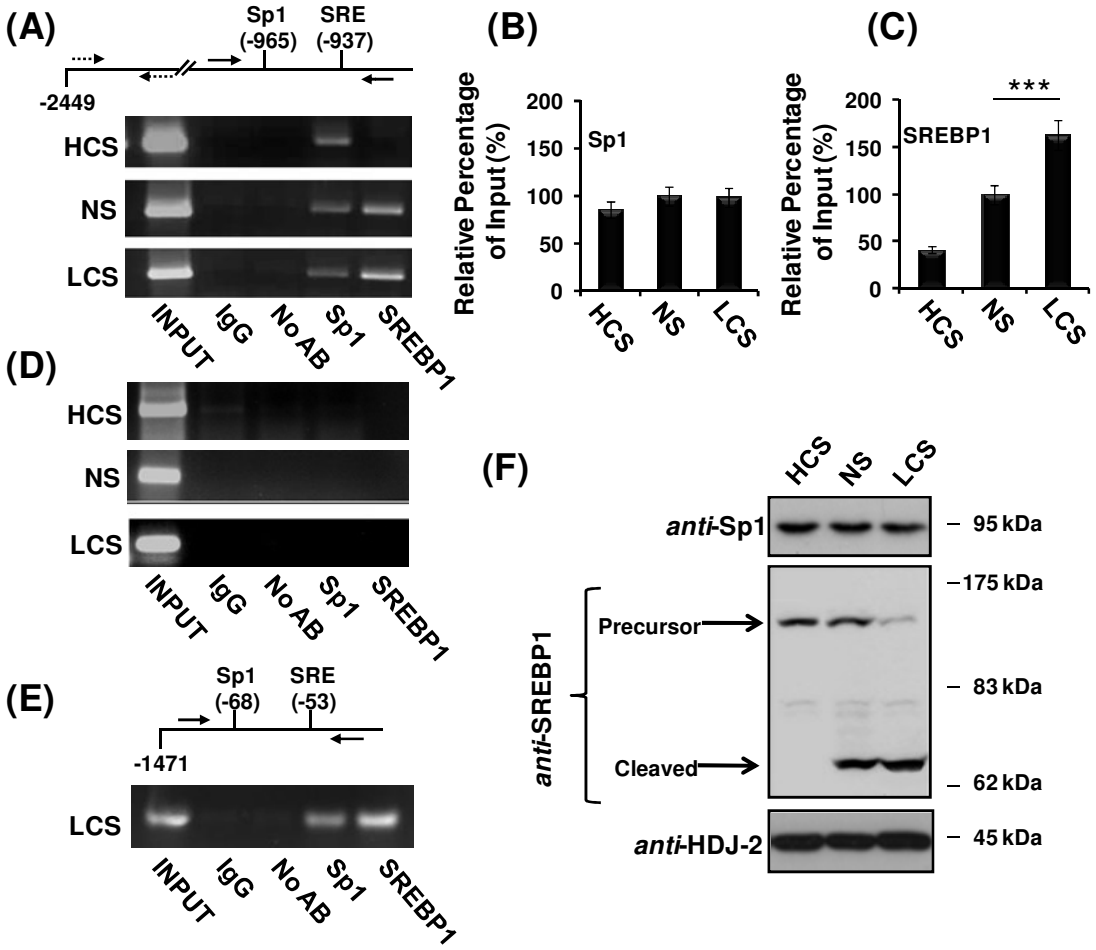

Figure 4: Chromatin immunoprecipitation (ChIP) analysis of SREBP1 binding to the proximal PrmIP region.

Panels A - D: ChIP analysis following culturing of EA.hy926 cells for 24 h in HCS, NS or LCS where the schematic above the panels shows the forward and reverse primers used to amplify either the cholesterol-responsive (-1271 to -772; solid arrows; **Panel A**) or, as controls, downstream (-1901 to -1540; dashed arrows; **Panel D**) sub-fragments of the PrmIP genomic region from immunoprecipitates of the cross-linked chromatin. Images are representative of three independent experiments. The bar charts shows real time quantitative RT-PCR analysis of the ChIP data in Panel A, where mean levels of PCR product generated from the Sp1 (**Panel B**) and SREBP1 (**Panel C**) immunoprecipitates are expressed as a percentage relative to those levels derived from the corresponding input chromatins, as indicated. Data was obtained from three independent experiments (n = 3), where the levels in NS-cultured EA.hy926 cells is set to 100 %. **Panel E**: ChIP analysis of Sp1 and SREBP1 binding to the cholesterol-responsive LDL receptor promoter following culturing of EA.hy926 cells for 24 h in LCS, where the schematic above the panel shows the forward and reverse primers used (-124 to +55; solid arrows). Images are representative of three independent experiments. **Panel F**: Immunoblot analysis of Sp1, SREBP1 and HDJ-2 expression in EA.hy926 cells cultured for 24 h in NS, HCS or LCS, as indicated.

Figure 5

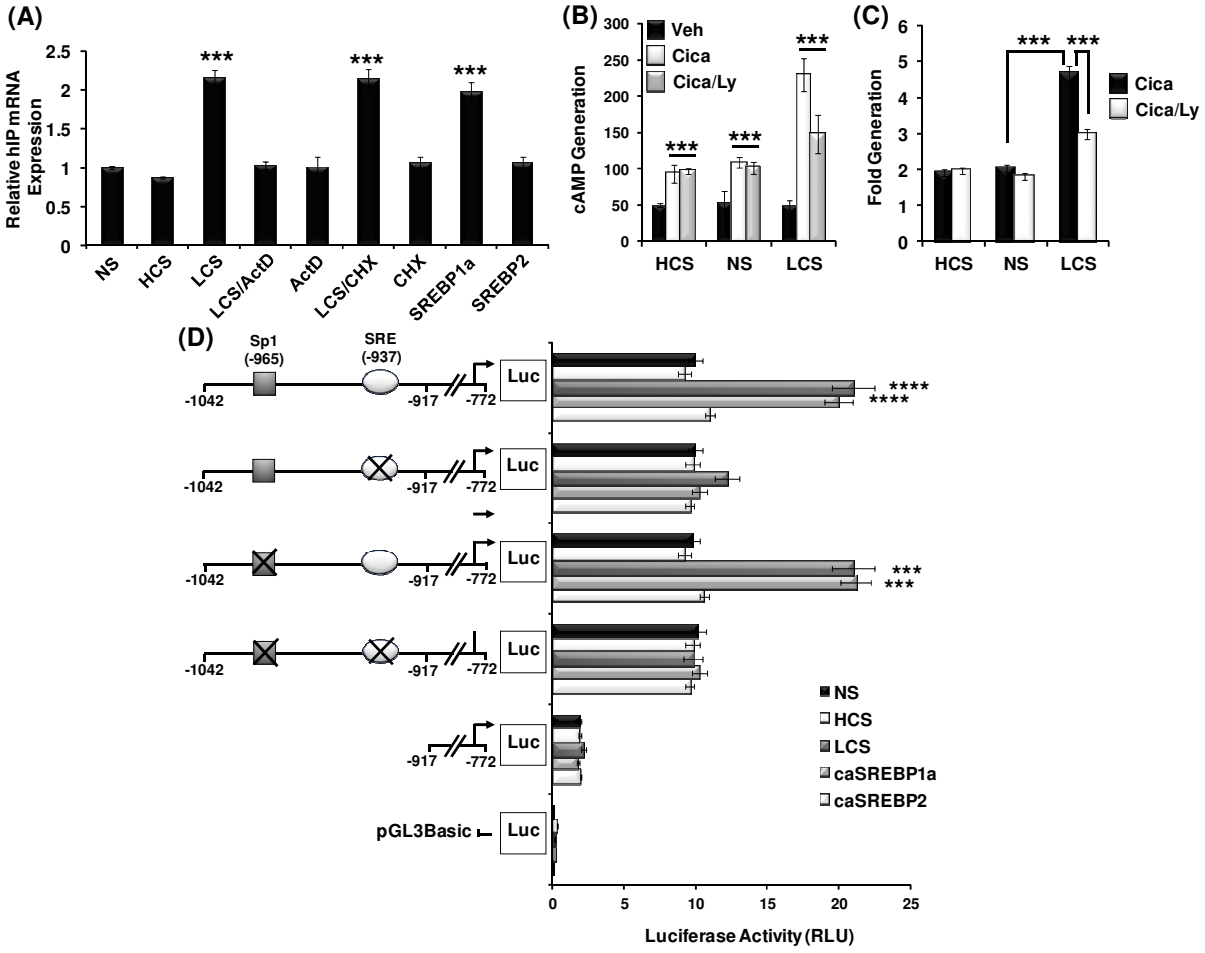
(A)
Relative hIP mRNA Expression
NS
HCS
LCS
LCS/ActD
ActD
LCS/CHX
CHX
SREBP1a
SREBP2
(B)
cAMP Generation
Veh
Cica
Cica/Ly
HCS
NS
LCS
(C)
Fold Generation
Cica
Cica/Ly
HCS
NS
LCS
(D)
Sp1 (-965)
SRE (-937)
-1042
-917
-772
Luc
pGL3Basic
NS
HCS
LCS
caSREBP1a
caSREBP2
Luciferase Activity (RLU)

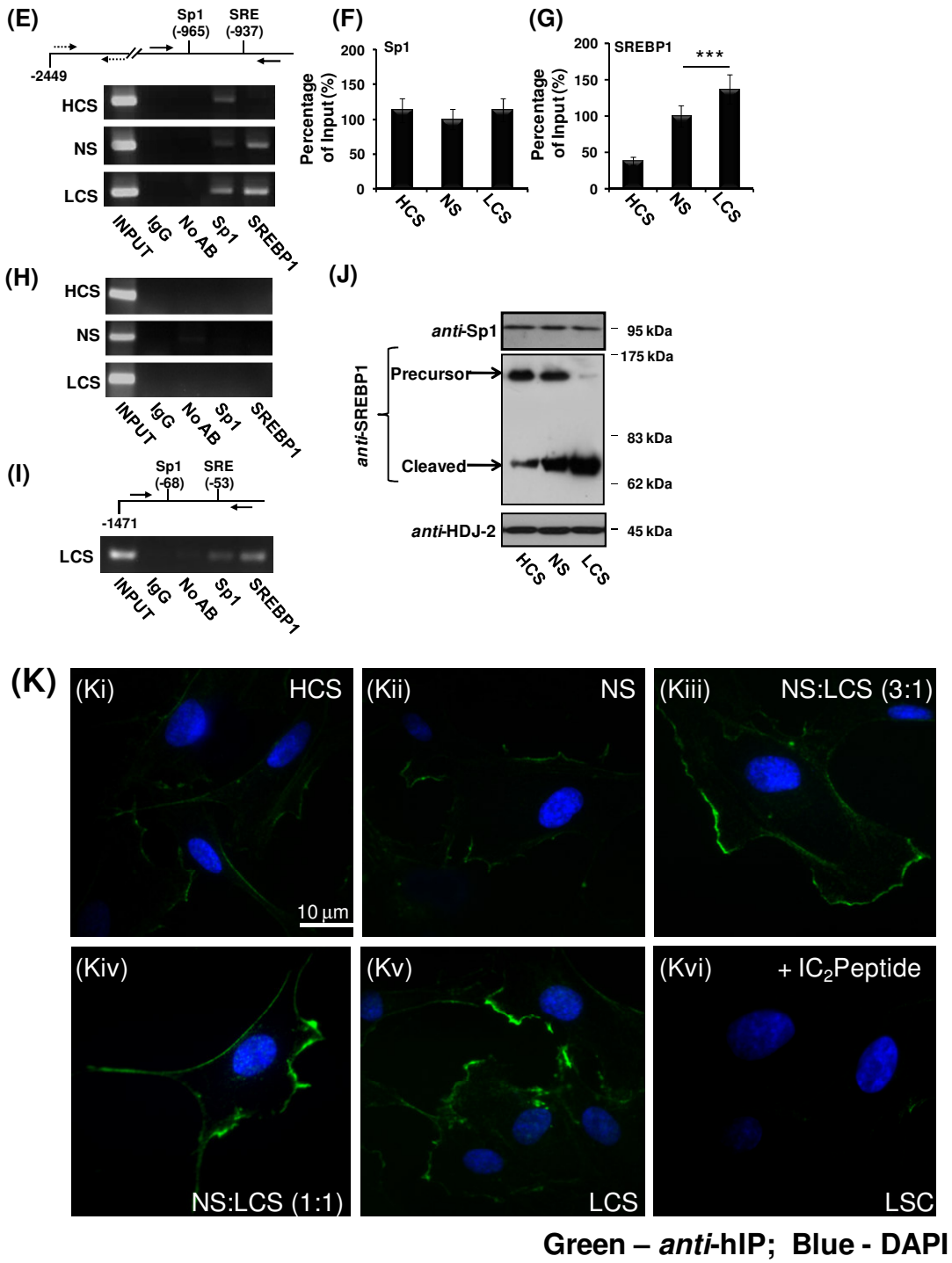

Figure 5: Cholesterol regulation of hIP expression in 1° HUVECs.
Panel A: Real-time quantitative RT-PCR analysis of hIP relative to GA3'PDH mRNA expression in 1° HUVECs cultured for 24 h in either NS, HCS or LCS, and/or ActD (10 µg/ml), CHX (20 µg/ml) or transfected with vectors encoding SREBP1a^{-460} and SREBP2^{-468}, as indicated. **Panels B & C**: **1° HUVECs** were co-transfected with pCRE-Luc; 24 h post-transfection, media was replaced with fresh NS, HCS or LCS media in either the absence or presence of Ly294002 (Ly; 20 µM) and cells were cultured for an additional 24 h. For measurement of agonist-induced cAMP generation, cells were stimulated for 3 h with cicaprost (1 µM) or, as controls, with the drug vehicle (V; PBS). Data is presented as hIP-induced cAMP accumulation (**Panel B**: RLU ± SEM, n =3) or as fold-inductions in

hIP-induced cAMP accumulation in LCS relative to NS-cultured cells (**Panel C**). **Panel D**: Effect of ectopic expression of SREBP1a^{-460} and SREBP2^{-468} on PrmIP-directed luciferase gene expression in 1^{o} HUVECs cultured for 24 h in NS, HCS, or LCS (RLU ± SEM; n = 6). The asterisks (*) indicate where cholesterol depletion in LCS resulted in significant changes in either hIP mRNA, PrmIP-directed gene expression or cAMP generation relative to those levels in NS, where *, ***, and **** indicates $p < 0.05$, $p < 0.001$ and $p < 0.0001$, respectively, for post-hoc Dunnett's multiple comparison *t*-test analysis. **Panels E-H:** ChIP analysis following culturing of 1^{o} HUVECs for 24 h in HCS, NS or LCS where the schematic above the panels shows the forward and reverse primers used to amplify either the cholesterol-responsive (-1271 to -772; solid arrows; **Panel E**) or, as controls, downstream (-1901 to -1540; dashed arrows; **Panel H**) sub-fragments of the PrmIP genomic region from immunoprecipitates of the cross-linked chromatin. Images are representative of three independent experiments. The bar charts shows real time quantitative RT-PCR analysis of the ChIP data in Panel E, where mean levels of PCR product generated from the Sp1 (**Panel F**) and SREBP1 (**Panel G**) immunoprecipitates are expressed as a percentage relative to those levels derived from the corresponding input chromatins, as indicated. Data was obtained from three independent experiments (n = 3), where the levels in NS-cultured 1^{o} HUVECs is set to 100 %. **Panel I**: ChIP analysis of Sp1 and SREBP1 binding to the cholesterol-responsive LDL receptor promoter following culturing of 1^{o} HUVECs for 24 h in LCS, where the schematic above the panel shows the forward and reverse primers used (-124 to +55; solid arrows). Images are representative of three independent experiments. **Panel J**: Immunoblot analysis of endogenous Sp1, SREBP1 and HDJ-2 expression in 1^{o} HUVECs cultured for 24 h in NS, HCS or LCS where blots were screened with *anti*-Sp1, *anti*-SREBP1 or *anti*-HDJ antisera, as indicated. Images are representative of three independent experiments. **Panel K:** Immunofluorescence microscopy of 1° HUVECs cultured for 24 h in either (**Ki**)HCS, (**Kii**) NS, (**Kiii**) NS:LCS, 3:1; (**Kiv**) NS:LCS, 1:1 or (**Kv**) LCS and immunolabelled with *anti*-hIP sera and Alexa Fluor 488-conjugated *anti*-rabbit IgG (green), followed by counterstaining with DAPI (blue). Bottom right image in **Panel Kvi**: Immunoscreening of 1° HUVECs cultured in LCS with *anti*-hIP antibody pre-incubated with the antigenic peptide directed to IC_2 of the hIP (10 μg/ml). Data shown are averages of 10 fields per condition of three independent experiments (n = 30 fields per condition). Images were captured at 63x magnification using a Zeiss microscope and Axiovision software.

Figure 6

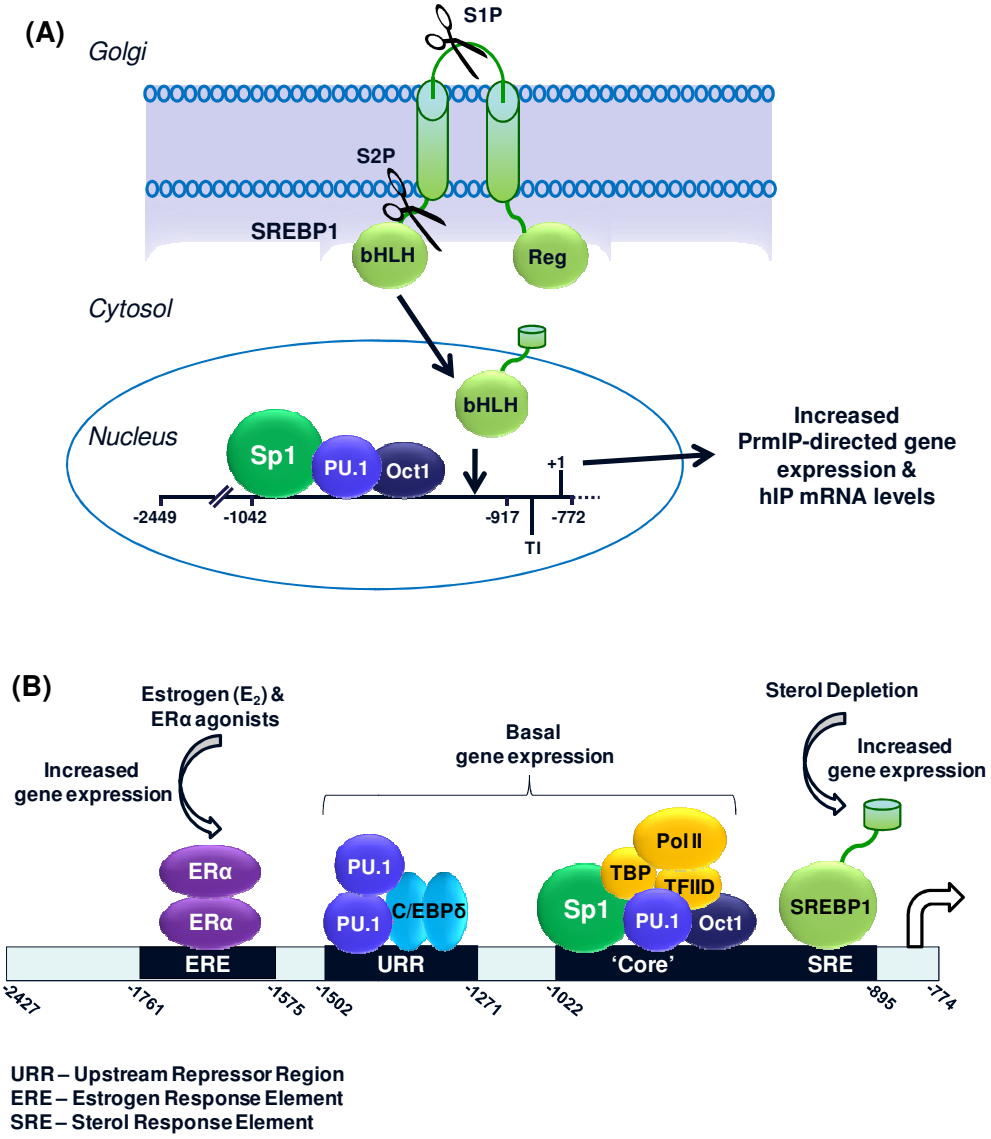

Figure 6: Panel A: Model of SREBP1-regulation of hIP expression. During cholesterol-depletion, when the cellular level of sterols drops, the SREBP1a precursor protein is transported to the Golgi apparatus, where it is first cleaved by site-1 protease (S1P) (scissors) and then by S2P (scissors). The liberated, transcriptionally active basic helix-loop-helix leucine-zipper (bHLH-LZ) domain of SREBP1a travels to the nucleus and directs the transcription of target genes through binding to SREs within their specific promoter regions. Herein, it was established that both hIP mRNA levels and PrmIP-directed gene expression are significantly increased in low serum cholesterol through a transcriptional mechanism involving binding of Sp1 and SREBP1a, but not SREBP2, to their adjacent consensus elements within the 'core' PrmIP. **Panel B: Transcriptional regulation of the human prostacyclin receptor (hIP) gene.** Schematic of the promoter region (PrmIP) of the hIP receptor gene. Along with other general components (e.g., RNA polymerase II, TBD, and TFIID) of the transcriptional apparatus, Sp-1, PU.1, Oct-1 and C/EBPδ are recognized *trans*-acting factors that regulate expression of the hIP under basal conditions (40,41). In addition, also shown in the schematic are the evolutionary conserved estrogen response element (ERE) and sterol response element (SRE), which participate in direct ERα-dependent and SREBP1-dependent induction of hIP gene expression in response to estrogen (32) and low-serum cholesterol, respectively.

SUPPLEMENTAL FIGURES

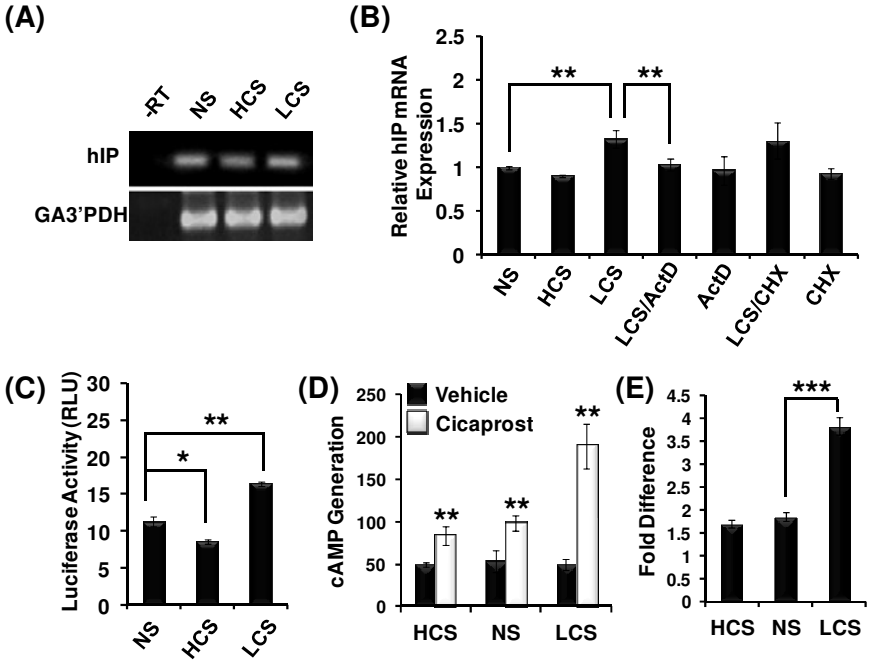

Supplemental Figure 1: Effect of cholesterol on hIP mRNA, PrmIP-directed gene expression and hIP-induced cAMP generation in HEL 92.1.7 cells.
RT-PCR (**Panel A**) and real-time quantitative RT-PCR (**Panel B**) analysis of hIP relative to GA3'PDH mRNA expression in HEL 92.1.7 cells cultured for 24 h in either NS, HCS, LCS, and/or ActD (10 μg/ml) and CHX (20 μg/ml) as indicated. **Panel C**: HEL 92.1.7 cells were co-transfected with pGL3B:PrmIP plus pRL-TK; 24 h post-transfection media was replaced with NS, HCS or LCS and cells were cultured for an additional 24 h prior to measurement of PrmIP-directed luciferase reporter gene expression (RLU ± SEM; n = 6). Data is presented as mean firefly relative to renilla luciferase activity, expressed in arbitrary relative luciferase units (RLU ± SEM; n = 6). **Panels D & E**: HEL cells were co-transfected with pCRE-Luc; 24 h post-transfection, media was replaced with fresh NS, HCS or LCS media and cells were cultured for an additional 24 h. For measurement of agonist-induced cAMP generation, cells were stimulated for 3 h with cicaprost (1 μM) or, as controls, with the drug vehicle (V; PBS). Data is presented as hIP-induced cAMP accumulation (**Panel D**: RLU ± SEM, n =3) or as fold-inductions in hIP-induced cAMP accumulation in LCS relative to NS-cultured cells (**Panel E**). The asterisks (*) indicate where cholesterol depletion in LCS resulted in significant changes in either hIP mRNA, PrmIP-directed gene expression or cAMP generation relative to those levels in NS, where *, ***, and **** indicates $p < 0.05$, $p < 0.001$ and $p < 0.0001$, respectively, for post-hoc Dunnett's multiple comparison *t*-test analysis.

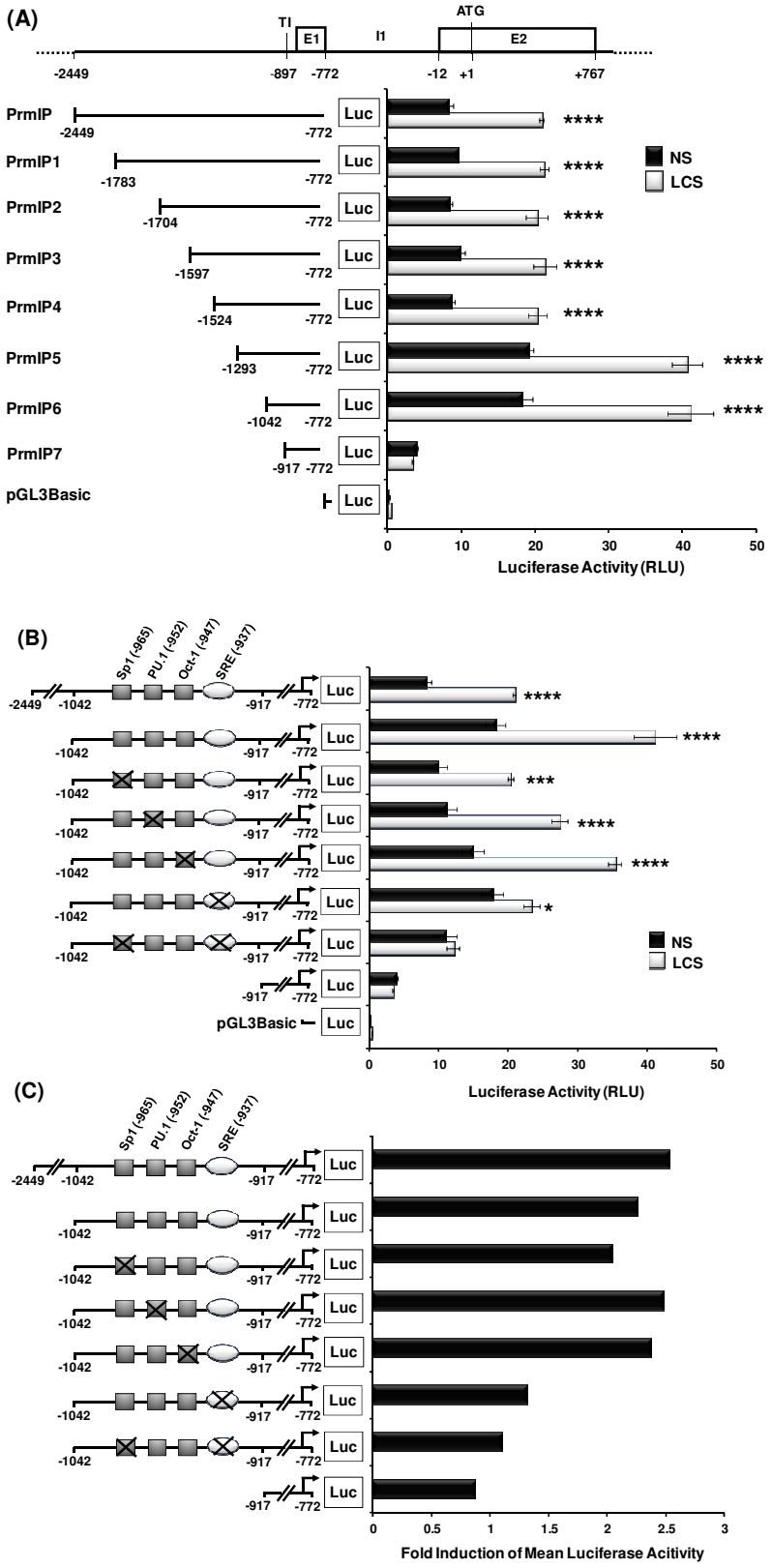
(A)
TI
E1
I1
ATG
E2
-2449
-897
-772
-12
+1
+767
PrmIP
PrmIP1
PrmIP2
PrmIP3
PrmIP4
PrmIP5
PrmIP6
PrmIP7
pGL3Basic
Luc
-1783
-1704
-1597
-1524
-1293
-1042
-917
****
NS
LCS
0
10
20
30
40
50
Luciferase Activity (RLU)
(B)
Sp1 (-965)
PU.1 (-952)
Oct-1 (-947)
SRE (-937)
***
*
(C)
0
0.5
1
1.5
2
2.5
3
Fold Induction of Mean Luciferase Acitivity

Supplemental Figure 2: Identification of a putative SRE within PrmIP.
Panels A: Localisation of the cholesterol-responsive region within PrmIP by 5' deletion analysis. A schematic of the hIP genomic region, spanning nucleotides -2449 to +767, encoding PrmIP, exon (E)1, intron (I)1 and E2, where +1 corresponds to the translational start site. PrmIP-, PrmIP1-, PrmIP2-, PrmIP3-, PrmIP4-, PrmIP5-, PrmIP6- and PrmIP7-directed luciferase gene expression in HEL 92.1.7 cells cultured for 24 h in NS or LCS (RLU ± SEM; n = 6). **Panels B & C:** A schematic of PrmIP6 in addition to the putative Sp1, PU.1, Oct-1 and SRE binding sites, where the 5' nucleotide of each *cis*-acting element is indicated in brackets (-965, -952, -947 and -937, respectively). PrmIP6, PrmIP6^{SP1*}, PrmIP6$^{PU.1*}$, PrmIP6$^{Oct\text{-}1*}$, PrmIP6^{SRE*}, PrmIP6$^{SRE/Sp1*}$and PrmIP7-directed luciferase expression in HEL 92.1.7 cells cultured for 24 h with either NS or LCS. Data is **Panels A & C** is presented as mean firefly relative to renilla luciferase activity expressed in arbitrary relative luciferase units (RLU ± SEM; n = 6) or in **Panel D** as fold induction of mean luciferase activity in LCS- relative to that in NS-cultured cells. The asterisks (*) indicate where culturing cells in LCS led to significant increases in luciferase expression in HEL 92.1.7 cells relative to that in NS, where *, ***, and **** indicates $p < 0.05$, $p < 0.001$ and $p < 0.0001$, respectively, for post-hoc Dunnett's multiple comparison *t*-test analysis.

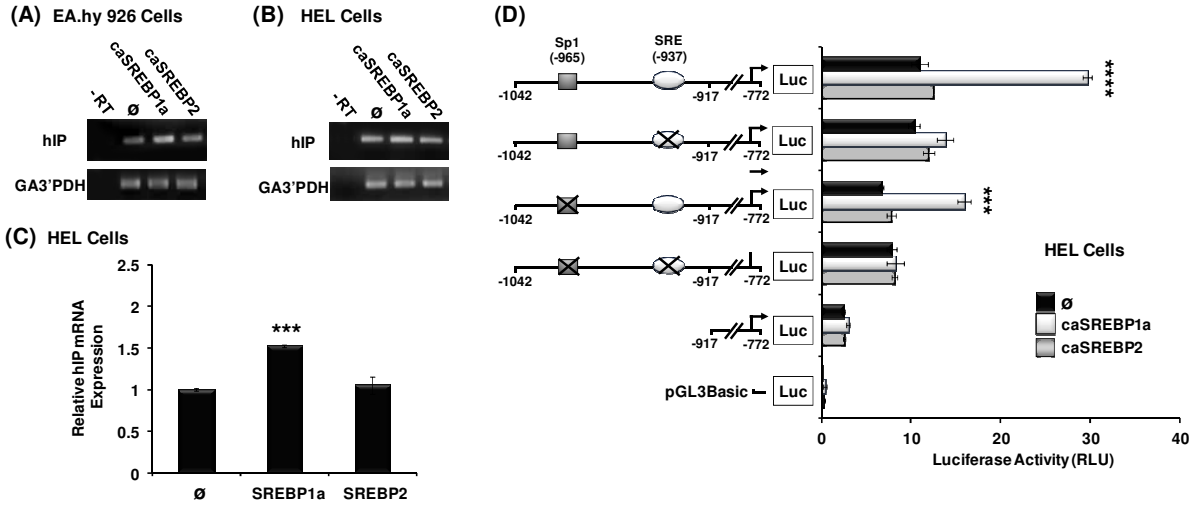

Supplemental Figure 3: Effect of SREBP ectopic expression on hIP mRNA and PrmIP-directed gene expression in EA.hy926 and HEL 92.1.7 cells.
RT-PCR (**Panels A & B**) and real-time quantitative RT-PCR (**Panel C**) of the effect of ectopic expression of constitutively active SREBP1a^{-460} or SREBP2^{-468} on hIP relative to GA3'PDH mRNA expression in EA.hy926 (**Panel A**) and HEL 92.1.7 (**Panels B & C**) cells and on PrmIP -directed luciferase expression in HEL 92.1.7 cells (**Panel D**). The asterisks (*) in **Panels C & D** indicate where ectopic expression of SREBP1a^{-460} significantly increased either hIP mRNA or PrmIP-directed gene expression where *** and **** indicates $p < 0.001$ and 0.0001, respectively, for post-hoc Dunnett's multiple comparison *t*-test analysis.

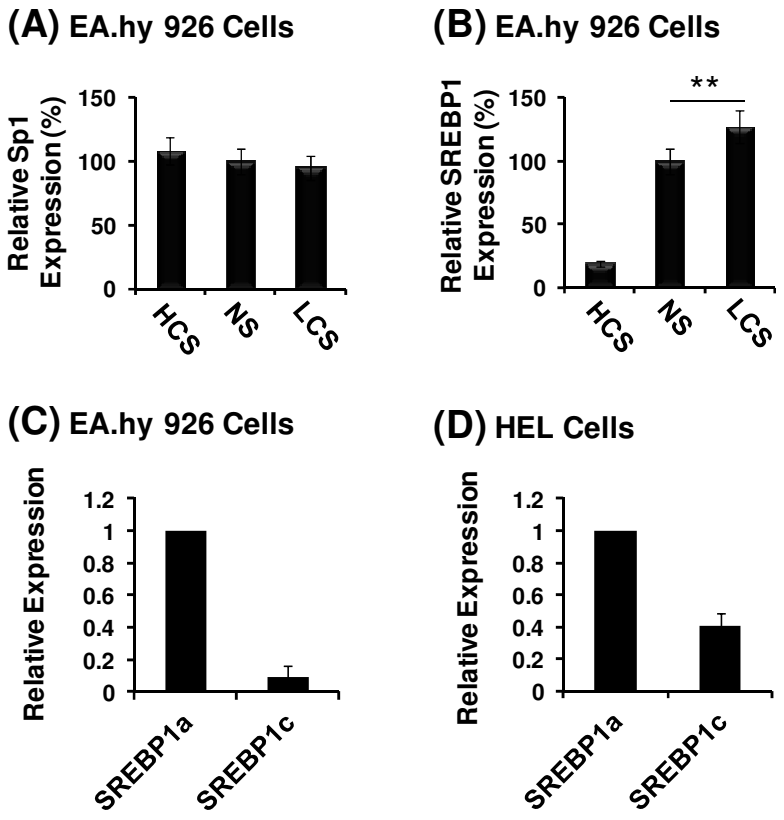

Supplemental Figure 4: Quantitation of SREBP1 and Sp1 expression in EA.hy926 and HEL cells.

Panels A & B: Densitometry analysis of Sp1 (**Panel A**) and SREBP1 (**Panel B**) relative to HDJ-2 expression in EAhy926 cells cultured for 24 h in either NS, HCS or LCS, where the level in NS-cultured cells is set to 100 %. **Panels C & D**: real-time quantitative RT-PCR analysis of SREBP1a and SREBP1c mRNA expression in EAhy926 and HEL 92.1.7 cells, respectively, cultured in NS. Data was obtained from three independent experiments (n = 3), where the levels of SREBP1a are set to 1.

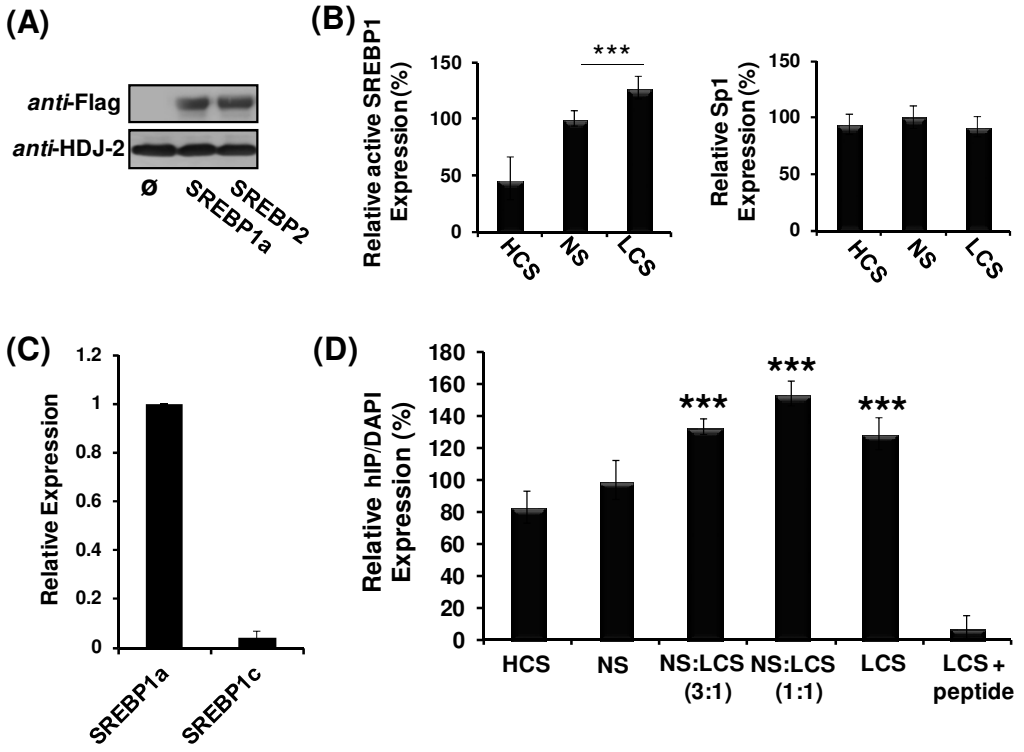

Supplemental Figure 5: Quantitation of SREBP expression in 1° HUVECs.
Panel A: Immunoblot analysis confirming over-expression of the FLAG-tagged SREBP1a^{-460} or SREBP2^{-468} proteins in 1° HUVECs, where secondary screening of membranes with *anti*-HDJ confirmed uniform protein loading. **Panel B**: Densitometry analysis (ImageJ software), where the bar charts represent the mean relative expression of SREBP1 (left) and Sp1 (right) relative to HDJ-2 protein expression in cells cultured for 24 h in either NS, HCS or LCS, where the level in NS-cultured cells is set to 100 %. **Panel C**: real-time quantitative RT-PCR analysis of SREBP1a and SREBP1c mRNA expression in 1° HUVECs cultured in NS. Data was obtained from three independent experiments (n = 3), where the levels of SREBP1a are set to 1. **Panel D:** Immunofluorescence microscopy of human IP expression in 1° HUVECs. The bar charts shows mean levels of hIP expression normalized against DAPI nuclear staining in 1° HUVECs cultured in NS, LCS or HCS as indicated (relative expression, % ± SEM, n = 4), where hIP expression in NS-cultured cells is set to 100 %. The asterisks (*) indicate that hIP expression was significantly increased in response to cholesterol depletion relative to NS-cultured cells where *** indicates $p < 0.001$, for post-hoc Dunnett's multiple comparison *t*-test analysis.